

This file has been cleaned of potential threats.

If you confirm that the file is coming from a trusted source, you can send the following SHA-256 hash value to your admin for the original file.

b72e2d20c1124f0c8c420b986097bccab00b93c2cb17c2a67f5c7e5cddd8eaea

To view the reconstructed contents, please SCROLL DOWN to next page.

The text that follows is a PREPRINT.
O texto que segue é um PREPRINT.

Please cite as:

Favor citar como:

Santos, Y.L.F., A.M. Yanai, C.J.P. Ramos,
P.M.L.A. Graça, J.A.P. Veiga, F.W.S. Correa
& P.M. Fearnside. 2022. **Amazon
deforestation and urban expansion:
Simulating future growth in the Manaus
Metropolitan Region, Brazil.** *Journal of
Environmental Management* 304: art.
114279.
<https://doi.org/10.1016/j.jenvman.2021.114279>

ISSN: 0301-4797

DOI: 10.1016/j.jenvman.2021.114279

Copyright: Elsevier

The original publication is available at:

O trabalho original está disponível em:

<https://doi.org/10.1016/j.jenvman.2021.114279>

<https://www.journals.elsevier.com/journal-of-environmental-management>

**Amazon Deforestation and Urban Expansion:
Simulating Future Growth in the Manaus Metropolitan Region, Brazil**

Yara L. F. SANTOS^{1,2}, Aurora M. YANAI⁴, Camila J. P. RAMOS³, Paulo M. L. A. GRAÇA⁴,
Jose A. P. VEIGA², Francis W. S. CORREA², and Philip M. FEARNSIDE⁴

¹Postgraduate program in Climate and the Environment, National Institute for Research in Amazonia (INPA), Av. André Araújo, 2936, CEP 69067-375, Manaus, Amazonas, Brazil

²Postgraduate program in Climate and the Environment, State University of Amazonas (UEA), Av. Darcy Vargas, 1200, CEP 69050-020, Manaus, Amazonas, Brazil

³Postgraduate program in Ecology, National Institute for Research in Amazonia (INPA), Av. André Araújo, 2936, CEP 69067-375, Manaus, Amazonas, Brazil

⁴Department of Environmental Dynamics, National Institute for Research in Amazonia (INPA), Av. André Araújo, 2936, CEP 69067-375, Manaus, Amazonas, Brazil

E-mail addresses: yarasantos88@gmail.com (Yara L. F. Santos), yanai@inpa.gov.br (Aurora M. Yanai), camilajramos@gmail.com (Camila J. P. Ramos), pmlag@inpa.gov.br (Paulo M. L. A. Graça), jveiga@uea.edu.br (Jose A. P. Veiga), fcorreia@uea.edu.br (Francis W. S. Correa), pmfearn@inpa.gov.br (Philip M. Fearnside)

1. Introduction

In 1950, with 54 million inhabitants, Brazil had the largest population in South America. Of this total, 36% of the inhabitants lived in urban areas. In 2019, Brazil still had the largest population in South America, with approximately 210 million inhabitants. Of this total, 99.8 million (48%) lived in integrated regions of development and/or urban agglomerations (IBGE, 2019a). According to the United Nations, by 2050 approximately 90% of the Brazilian population will reside in urban areas (United Nations, 2019).

Urban growth implies physical and functional changes due to the transition from rural to urban forms. This process consists of complex non-linear interactions among various components, including topography, rivers, land use/cover, transport, culture, population, economy, and infrastructure (Pavão, 2017). Moreover, the disorderly urban growth can cause a number of environmental and social problems. In the environmental sphere, for example, the following implications can be highlighted: 1) reduction and fragmentation of green areas with respective reduction of local fauna and flora (Allen, 2003; Ramos et al., 2018); 2) erosion and contamination of rivers and tributaries that can produce an environmental imbalance - eutrophication, reduction of biodiversity, waterborne diseases, among other effects (Fonseca et al., 2016; Costa et al., 2020; Paiva et al., 2020); 3) decrease in soil permeability that, consequently, can increase the occurrence of floods (Tucci, 2008); 4) increase in respiratory diseases as a result of the intensification of soil and air pollution (Ignotti et al., 2010) and; 5) increase in surface and air temperature, implying the so-called urban heat island effect (Kalnay & Cai, 2003; de Souza, & dos Santos Alvalá, 2014). In the social scenario we highlight the lack of housing that leads to the emergence of slums and/or the construction of housing in irregular locations, unemployment, increased violence and social exclusion (Allen, 2003; Souza, 2015).

In the Amazon, the urbanization process first occurred by rivers, which are an important transport route in the region (Sant'Anna, 1998; Resende, 2006; Kuwahara et al., 2012; Góes Filho, 2015). Most Amazonian cities are still located along rivers or in coastal areas (Costa, 2000). However, in the 1960s and 1970s, the Brazilian federal government started to build highways in the Amazon, such as the BR-230 (Transamazon Highway), BR-010 (Belém – Brasília), BR-319 (Manaus – Porto Velho), and the BR-174 (Manaus – Boa Vista). This facilitated agricultural, mineral, timber, and industrial projects in the region and consequently rural exodus from various parts of the country to urban centers in the Brazilian Amazon (Costa, 2000; Barbieri & Carr, 2005; Becker, 2005; Schor & Oliveira, 2011; Costa et al., 2019). Despite its low demographic density, the population in the Brazilian Amazon increased from around 8.2 million in 1970 to 24 million in 2010, a growth of 193% (IBGE, 2010). This population growth was concentrated in urban centers and became one of the largest environmental problems in the region due to rapid migration as well as a lack of planning and infrastructure (Becker, 2001).

The Manaus Metropolitan Region (MMR), created on May 30, 2007, has different characteristics from other Brazilian metropolitan regions (Guedes et al., 2009). The MMR is located in the center of the largest Brazilian biome – the Amazon biome (MMA, 2019). In this region, the municipal (county) seats are distant from each other, usually separated by the forest or rivers. Infrastructure, such as the Jornalista Phelippe Daou Bridge (the Rio Negro Bridge, opened in 2011), which connects Manaus to Iranduba, produced profound changes in land-use/cover in these municipalities. In the municipality of Iranduba, planned neighborhoods emerged and the Manuel Urbano highway (AM-070), connecting Manaus to

51 Iranduba, Manacapuru, and Novo Airão, was duplicated to form a divided highway. A peri-
52 urbanization process occurred in these municipalities, altering the physiognomy of their
53 landscapes. Peri-urban areas are characterized by having urban, rural, and natural elements at
54 different levels (Allen, 2003; Moreira et al., 2016). Ramos et al. (2018) analyzed the peri-
55 urbanization process on the right bank of the Rio Negro after the inauguration of the Rio
56 Negro Bridge and simulated deforestation up to 2030 in the municipalities of Iranduba,
57 Manacapuru, and Novo Airão. Their results show that the most vulnerable areas to
58 deforestation are those with the combination of ample available forest and an expanding road
59 network far from large urban centers.

60
61 Land-use change processes are expected to accelerate in the coming decades (Ritchie &
62 Roser, 2018). Thus, the increased migration to urban areas, housing scarcity, and insufficient
63 infrastructure require urban regions to constantly monitor and plan land-use change (Thapa &
64 Murayama, 2011a). Understanding how the urban growth process occurs in the MMR is
65 necessary because the few studies that exist focus only on the city of Manaus (Powell et al.,
66 2007; Imbiriba et al., 2009; Souza et al., 2016). In addition, the MMR's location in the
67 middle of a tropical forest makes this area relevant to biodiversity and ecosystem services at
68 the regional and global level. This region still has large areas of continuous forest; but the
69 new dynamics of land-use/cover change heighten the vulnerability of the Amazon. The
70 objective of this study is to investigate how land-use/cover change could occur in the MMR
71 up to the end of the 21st century, with an emphasis on urbanization.

72

73 **2. Material and Methods**

74 **2.1 Study Area**

75

76 The Manaus Metropolitan Region (MMR) encompasses 13 municipalities in the
77 Brazilian state of Amazonas: Autazes, Careiro, Careiro da Várzea, Iranduba, Itacoatiara,
78 Itapiranga, Manacapuru, Manaquiri, Novo Airão, Presidente Figueiredo, Rio Preto da Eva,
79 Silves, and Manaus (Fig. 1). These municipalities cover an area of 127,000 km², or 8% of the
80 state of Amazonas (IBGE, 2019b). Of the 13 municipalities, Manaus, the capital of the state,
81 is the largest urban area, with around 400 km², and approximately 82% of the total population
82 of the MMR. Manaus is the seventh most populous municipality in the country, with
83 approximately 2,182,763 inhabitants in 2019 and an annual population growth rate of 1.7%
84 (IBGE, 2019b).

85

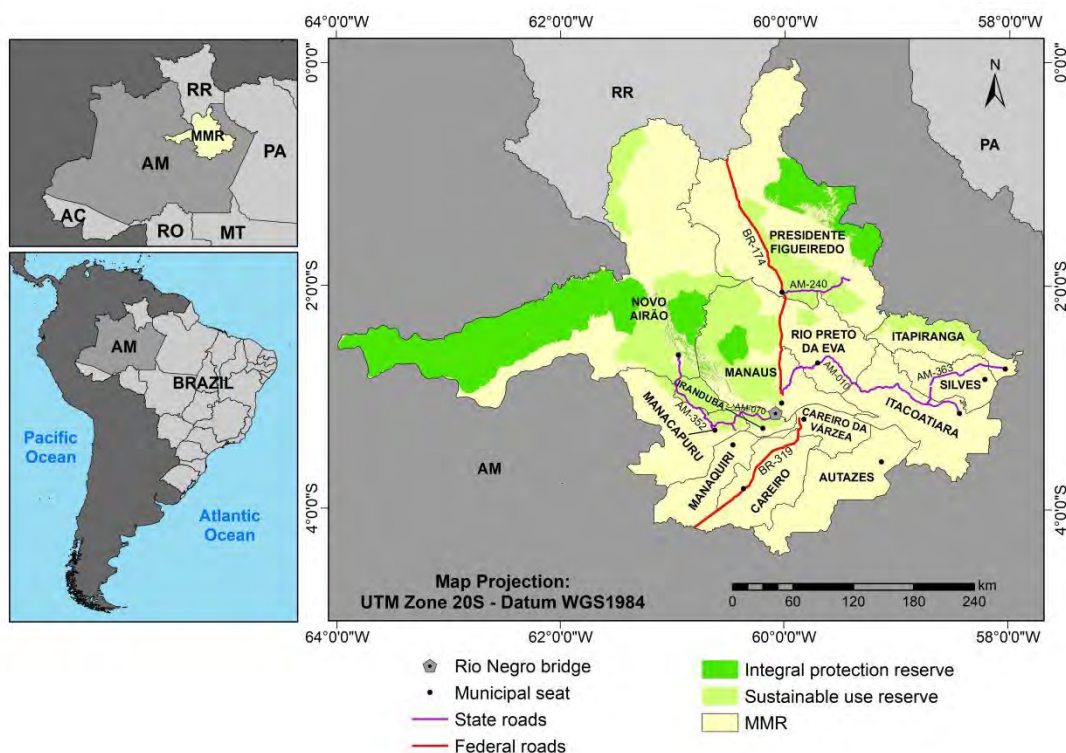


Fig. 1. Study area.

86

87 2.2 Spatial model of deforestation and urban expansion

88

89 To simulate deforestation and urban expansion in the MMR up to 2100, a spatial model
 90 of land-use/cover change used was developed in the environmental modeling platform
 91 Dinamica EGO (version 5.0.0). Dinamica EGO (Environment for Geoprocessing Objects) is
 92 free software developed by the Remote Sensing Center (CSR) of the Federal University of
 93 Minas Gerais (UFMG). It has been used to model land-use/cover change in the Amazon
 94 (Soares-Filho et al., 2002, 2006; Gonçalves, 2008; Fearnside et al., 2009; Yanai et al., 2012;
 95 Ramos et al., 2018; Osis et al., 2019), urban expansion and intra-urban dynamics (Almeida et
 96 al., 2003, 2008; Young, 2013), and fire propagation (Silvestrini et al., 2011; Soares-Filho et
 97 al., 2012; Brando et al., 2014, 2020; Faria et al., 2017).

98

99 Modeling in Dinamica EGO is of the cellular-automaton type. This means that to
 100 change the state of a cell (pixel) the model explicitly takes into account the state of
 101 neighboring cells following transition rules (Soares-Filho et al., 2002; Yeh & Li, 2006). All
 102 cells are evaluated simultaneously at each time step (Xie, 1996; Sirakoulis et al., 2000; Yeh
 103 & Li, 2006; Pontius Jr. et al., 2008).

104

105 The modeling steps consisted of (1) obtaining the input data, (2) calibrating and
 106 validating the model, and (3) simulating deforestation and urban expansion from 2017 to
 107 2100, based on a business-as-usual (BAU) scenario. In this scenario, the rates and spatial
 108 patterns of deforestation and expansion of urban areas in each municipality analyzed follow
 109 the trend observed from 2004 to 2010. This period includes the effect of the Rio Negro
 110 Bridge, including the planning period that began in early November 2003 and the bridge
 111 construction from its initiation in December 2007 until close to the inauguration of the bridge
 112 in October 2011. The effect of the bridge, especially in the municipalities of Iranduba and
 113 Manacapuru, was to an increase land speculation and the occupation of new areas, with the

114 potential for expanding deforestation and for driving socioeconomic transformations.
 115 Because the beginning of construction of the bridge in 2007 already led to increased real
 116 estate speculations and deforestation, a recent study used the period from 2008 to 2010 to
 117 assess the effect of bridge in a simulation of deforestation (Ramos et al., 2018).

118 119 2.3 Input data

120
121 In our model the cartographic data were in raster format with a spatial of 100 m, in
 122 which each cell had an area of 1 ha. The UTM (Universal Transverse Mercator) cartographic
 123 projection was used, corresponding to the UTM 20 South zone and Datum WGS 1984. The
 124 model used land-use/cover maps in the calibration (maps of 2004 and 2010), validation (2012
 125 and 2017), and simulation (2017-2100) stages.

126
127 Land-use/cover maps were based on data from the Amazon Deforestation Monitoring
 128 Project (PRODES) and the TerraClass project at the National Institute for Space Research
 129 (INPE) (Supplementary Material, Appendix 1). In the present study, the urban area class was
 130 derived from the TerraClass project (INPE, 2017) for 2004, 2010, and 2012. Due to the lack
 131 of TerraClass data for 2017, we used data from the previous years from TerraClass and
 132 updated the urban area with data from the classification made by the MapBiomias project
 133 (MapBiomias Project, 2018) and visual interpretation of satellite images from the Google
 134 Earth Pro program (Google Earth Pro, 2018). MapBiomias data were also used to reduce the
 135 loss of information in areas covered by clouds, identifying the classes of interest in these
 136 areas. Figure 2 presents a schematic of the methodology used to obtain land-use/cover map of
 137 the MMR for 2017.

138

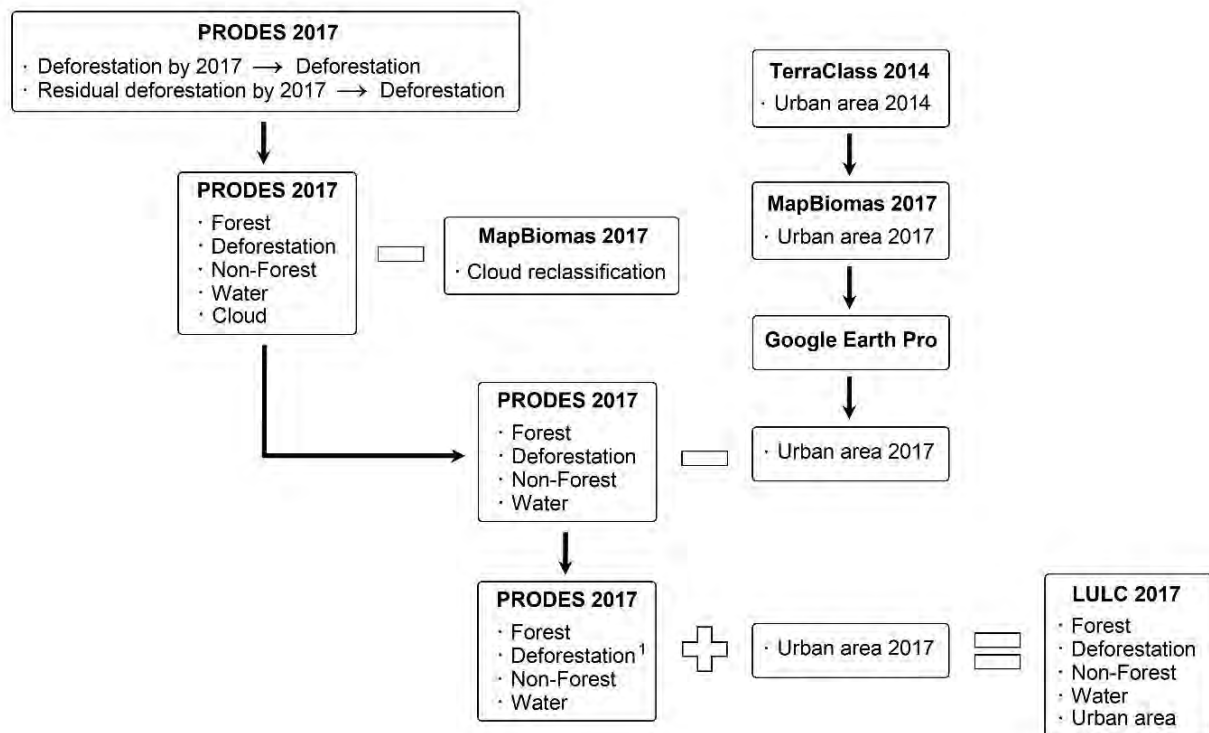


Fig. 2. Methodology for obtaining the 2017 land-use/cover map. The residual deforestation class corresponds to errors of omission in the PRODES mapping of previous years (Guerra et

al., 2010). Deforestation is the deforestation of PRODES without overlapping with the urban area.

139
140
141
142
143
144
145
146
147

In addition to the land-use/cover maps, other environmental spatial variables that influence deforestation and urban growth were required. The static variables used were elevation, slope, conservation units (protected areas for biodiversity), settlements (government-organized colonization projects for small farmers), quilombola areas (traditional territories of the descendants of escaped African slaves), indigenous lands, special areas (parks and military area), distance to rivers, distance to main highways, soil, and vegetation (Fig. 3). These variables do not change during model simulations.

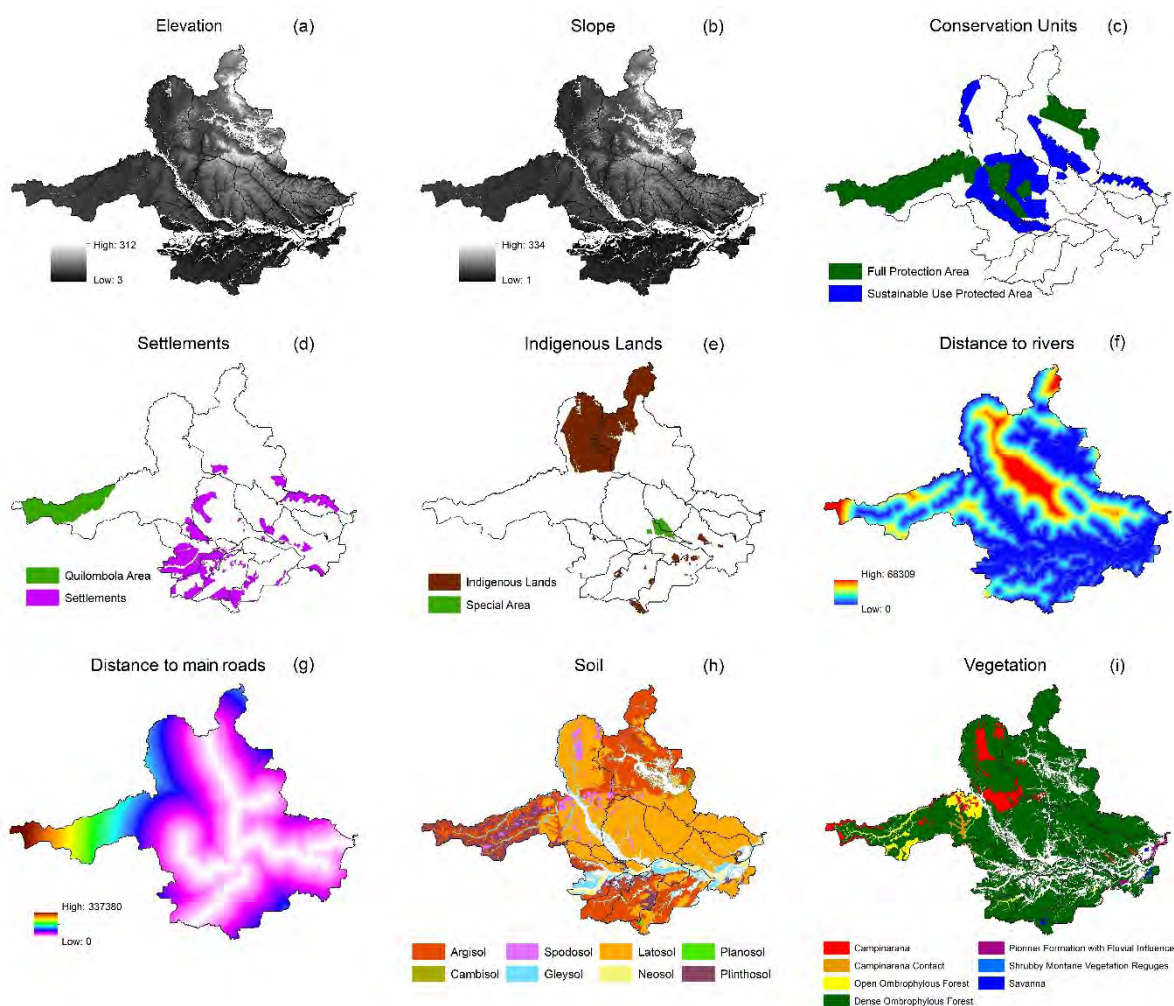


Fig. 3. Static variables used in the model: (a) Elevation, (b) Slope, (c) Conservation units, (d) Settlements and Quilombola Area, (e) Indigenous lands and Special areas, (f) Distance to rivers, (g) Distance to the main highways, (h) Soil, and (i) Vegetation. The distance and elevation variables are expressed in meters while the slope is in degrees.

148
149
150
151
152
153

The maps of distance to deforestation, distance to the urban area (central and non-central), and distance to secondary roads are considered to be dynamic variables because they are updated during the simulation. Distance to non-central urban areas are areas considered urban in the TerraClass project that are located away from the municipal seat. The dynamic variables and the maps of conservation units (protected areas for biodiversity), settlements

154 (areas where the government distributes parcels of lands to small farmers) and a quilombola
 155 area (an area traditionally occupied by descendants of escaped African slaves) were used to
 156 create the maps of the attractiveness and friction maps (see Supplementary Material,
 157 Appendix 2). The maps used as input for the model are described in Table 1.
 158

Table 1. Sources of maps prepared as input to the land-use/cover model.

Input data	Source
Land-use/cover maps (2004, 2010, 2012, and 2017)	<ul style="list-style-type: none"> ▪ PRODES – Amazon Deforestation Monitoring Project (PRODES, 2019); ▪ TerraClass is program complement to PRODES by adding information about land use and land cover in areas with clear-cutting mapped by PRODES (INPE, 2017); ▪ MapBiomass – MapBiomass Project – Collection 3 of the Annual Series of Land Coverage and Use Maps of Brazil (MapBiomass Project, 2018); ▪ Google Earth Pro (Google Earth Pro, 2018).
Maps of static variables	<ul style="list-style-type: none"> ▪ Elevation – SRTM – Shuttle Radar Topography Mission; ▪ Slope – EMBRAPA – Brazilian Agricultural Research Corporation; ▪ Conservation Units – MMA – Ministry of the Environment; ▪ Settlements – INCRA – National Institute for Colonization and Agrarian Reform; ▪ Quilombola Areas – INCRA – National Institute for Colonization and Agrarian Reform; ▪ Indigenous lands – FUNAI – National Indian Foundation; ▪ Soil – EMBRAPA – Brazilian Agricultural Research Corporation; ▪ Vegetation – IBGE – Brazilian Institute for Geography and Statistics; ▪ Distance from rivers* – PRODES – Amazon Deforestation Monitoring Project.
Maps of dynamic variables	<ul style="list-style-type: none"> ▪ Distance to deforestation* – PRODES; ▪ Distance to the urban area* – TerraClass and MapBiomass; ▪ Distance to the nearest non-central urban area* – TerraClass and MapBiomass; ▪ Distance to highways and secondary roads* – DNIT – National Department of Transport Infrastructure, IBGE – Brazilian Institute for Geography and Statistics and – United States Geological Survey – USGS – by visual interpretation of satellite images.

*The distance was calculated using a “Calc to Distance Map” functor in Dinamica EGO.

159

160 2.4 Model calibration and validation

161

162 The land-use/cover change model was regionalized according to municipal limits.
 163 Thus, each municipality has its own parameters for the amount of area to be deforested and
 164 the urban area to be expanded. Transition rates were calculated for changes in the status of
 165 the forest to deforestation and for deforestation to urban areas (Supplementary Material,
 166 Table S-2). The period from 2004 to 2010 was used in the calibration phase, and 2012 to
 167 2017 for the model validation.

168

169 In this study, we considered the annual rates of transitions from forest to deforestation
 170 and deforestation to urban areas. The deforestation rate for year “t” is multiplied by the extent

171 of the remaining forest in year “ $t - 1$ ” to obtain the area to be deforested in year “ t ” (Soares-
172 Filho et al., 2009). The same procedure was employed for the urban growth rate.

173

174 Dinamica EGO features two algorithms for spatial allocation of the status changes
175 produced by the expander and patcher transition functions. The expander function represents
176 the expansion of previously existing patches, while the patcher function creates new patches
177 through a seeding mechanism in which an initial set of pixels is generated to form new
178 patches (Soares-Filho et al., 2002). We established that 20% of the transition from forest to
179 deforestation would be in expander mode and the remainder in patcher mode. To better
180 represent the expansion pattern of the urban area, we established that 90% of the transition
181 from deforestation to urban area would be in the expander mode.

182

183 The calculation of transition probability maps employed the statistical weight of
184 evidence method. The transition probability maps present the most favorable areas for a
185 transition to occur, for example, from forest to deforestation (Soares-Filho et al., 2002). To
186 apply the weights-of-evidence method, the static and dynamic variables must be independent
187 of each other (Bonham-Carter et al., 1989). The analysis of the correlation between the
188 variables employed tests in pairs based on the Cramer coefficient and the Joint Information
189 Uncertainty. In this study, values above 0.5 were considered as dependent variables
190 (Bonham-Carter, 1994). When this occurs, one of the two variables must either be ignored or
191 the two must be combined into a third variable (Soares-Filho et al., 2009). In this study, the
192 environmental variables – conservation units and special areas (forest reserves and military
193 areas) – showed a correlation in most municipalities of the MMR. Thus, a third map
194 combining these variables was created. In addition, the municipality of Itacoatiara showed a
195 correlation between the dynamic variables “distance to the central urban area” and “distance
196 to non-central urban areas;” in this case we decided to keep the variable “distance to central
197 urban areas” because it has a more significant correlation with changes in land use/cover than
198 did “distance to non-central urban areas.”

199

200 The model was validated using the reciprocal similarity comparison technique that was
201 developed by Soares-Filho et al. (2009) from an adaptation of the fuzzy similarity method
202 (Hagen, 2003). The similarity between maps (observed and simulated) can range from 0% to
203 100%, where 0% indicates that the maps are completely different from each other and 100%
204 indicates that they are identical (Soares-Filho et al., 2009; Walker et al., 2010). As a result,
205 two values are obtained, 'minimum similarity' and 'maximum similarity'. This is because two
206 comparisons are made, one based on the observed map and the other based on the simulated
207 map, which can result in two similarity rates, a higher and a lower one. In this study, we
208 adopt the minimum similarity value as the reference. The parameter used to assess similarity
209 was set to constant decay, where a value of 1 refers to the similarity value if the
210 corresponding cells are found in the search window, and zero if they are not found (Soares-
211 Filho et al., 2009). In this approach, values above 50% similarity are considered satisfactory
212 for validation of a model (Ximenes et al., 2008; Vitel et al., 2009; Thapa & Murayama,
213 2011b; Yanai et al., 2012; Barni et al., 2015; Ramos et al., 2018; Osis et al., 2019).

214

215 Validation was carried out from a simulation for the period from 2012 to 2017 with
216 transition rates and weights-of-evidence coefficients for the period from 2004 to 2010. We
217 chose a validation period different from the calibration period to avoid the spurious effect of
218 using the same transition rates in these two stages (Paegelow et al., 2018). In addition to the
219 validation for 2017, we also compared our results with a null model. In this model, the same
220 input maps and transition rates were used, but the coefficients of the weight s-of-evidence

221 have been set to zero. This process generates random probability maps for each simulated
 222 year. In other words, the probability of a transition occurring is 50% (Soares-Filho, 2015;
 223 Osis et al., 2019). A summary of the settings used in this study is available in the
 224 Supplementary Material (Table S-3 and Appendix 3).

225

226 3. Results

227 3.1 Validation of the model

228

229 The minimum similarity values as a function of the number of windows are presented in
 230 Figure 4. The larger the size of the windows, the greater the similarity between the observed
 231 and simulated maps. The highest similarity values occurred for the 2017 simulations in non-
 232 random mode. This indicates that the adjustments made in the calibration represent an
 233 improvement in the spatial distribution of the simulated deforestation and in the urban
 234 expansion patches as compared to the null model in which the transitions occur in a random
 235 manner (Osis et al., 2019). The values of minimum similarity for the non-random simulation
 236 ranged from 17.4% (1×1 window) to 79.0% (19×19 window). For the 2017 simulation, in the
 237 random condition, the minimum similarity values ranged from 8.2% (1×1 window) to 50.7%
 238 (19×19 window). The 2017 simulations, in non-random mode, reached acceptable values
 239 (above 50%) in the seventh window (0.7 km of resolution).

240

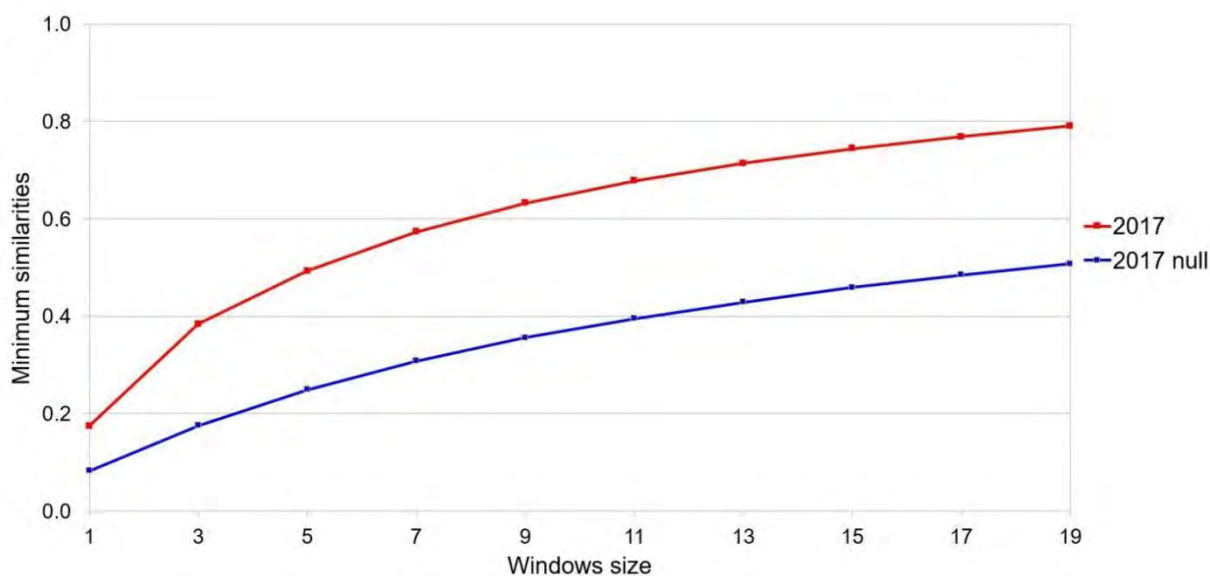


Fig. 4. Minimum values of fuzzy similarity with multiple resolution adjustment using the constant decay function. “Window size” is the number of cells (pixels) on each side of the square window area.

241 The observed and simulated maps of land-use/cover for the year 2017, with the urban
 242 area of Manaus centralized, are displayed in Figure 5. Note that the model adequately
 243 represented the change in land-use/cover in the region presented.

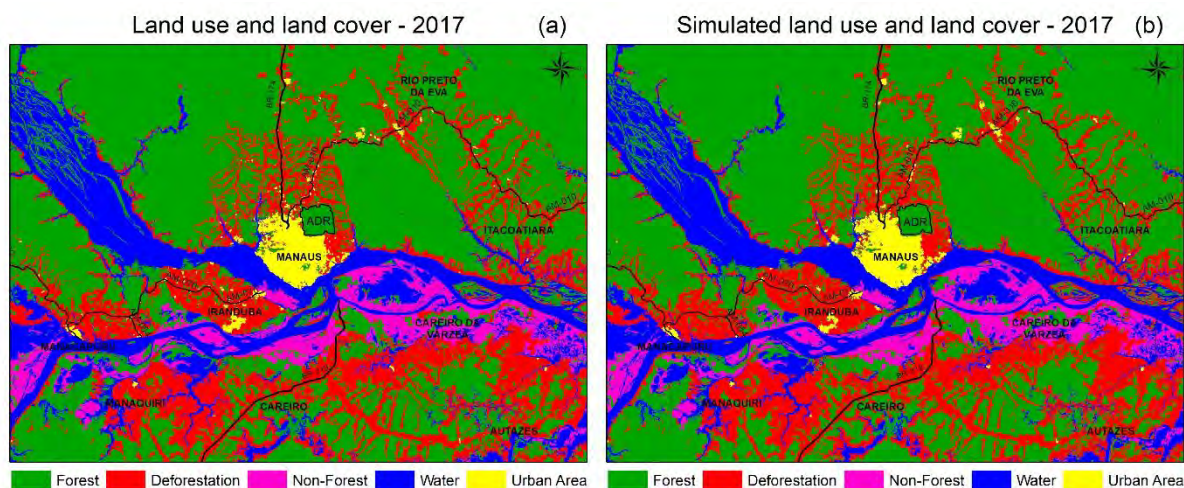


Fig. 5. Expanded detail comparing the observed and simulated land use maps for 2017, with emphasis on the Adolfo Ducke Reserve (ADR) area located in the urban area of Manaus (in the center).

244

245 The land-use/land-cover data from observed and simulated maps for the MMR, for the
 246 year 2017, as well as their percentage differences are presented in Table 2. The total
 247 percentage difference between the maps has an absolute value of 7.2%. The forest class
 248 showed the smallest percentage difference. The model overestimated the deforestation class
 249 and underestimated the forest and urban area classes.

250

Table 2. Land-use/land-cover data for the MMR in 2017 from observed and simulated maps.

Area (km ²) – 2017				
Class	Observed	Simulated	Absolute difference (simulated map – observed map)	Percentage difference (%)
Forest	99,115.5	98,703.4	-412.0	-0.4
Deforestation	11,227.8	11,655.5	427.8	3.8
Urban	525.7	510.0	-15.7	-3.0

251 Figure 6 charts the differences between the simulated and observed maps, for each
 252 municipality of the MMR in 2017. For the deforestation class (red bars), the model achieved
 253 percentage differences of less than 10% between the observed and simulated maps. For this
 254 class, the municipality of Novo Airão had the smallest percentage difference (-0.1%). The
 255 municipalities of Manaus and Rio Preto da Eva both showed percentage differences of less
 256 than 1%. On the other hand, the municipality of Itapiranga exhibited the largest percentage
 257 difference (9.4%). For the urban class (blue bars), the model displayed greater differences
 258 between the simulated map and the observed map. The municipality of Careiro da Várzea had
 259 a relatively high percentage difference (-64.5%) for the urban area, while the municipality of
 260 Manaus had the smallest percentage difference (-0.2%). More than half of the municipalities
 261 (Autazes, Careiro, Itacoatiara, Manaus, Novo Airão, Presidente Figueiredo and Rio Preto da
 262 Eva) showed a difference below 10%. Note that the denominators from which these
 263 percentages are calculated vary widely among the municipalities, with Manaus having by far
 264 the largest initial urban area.

265

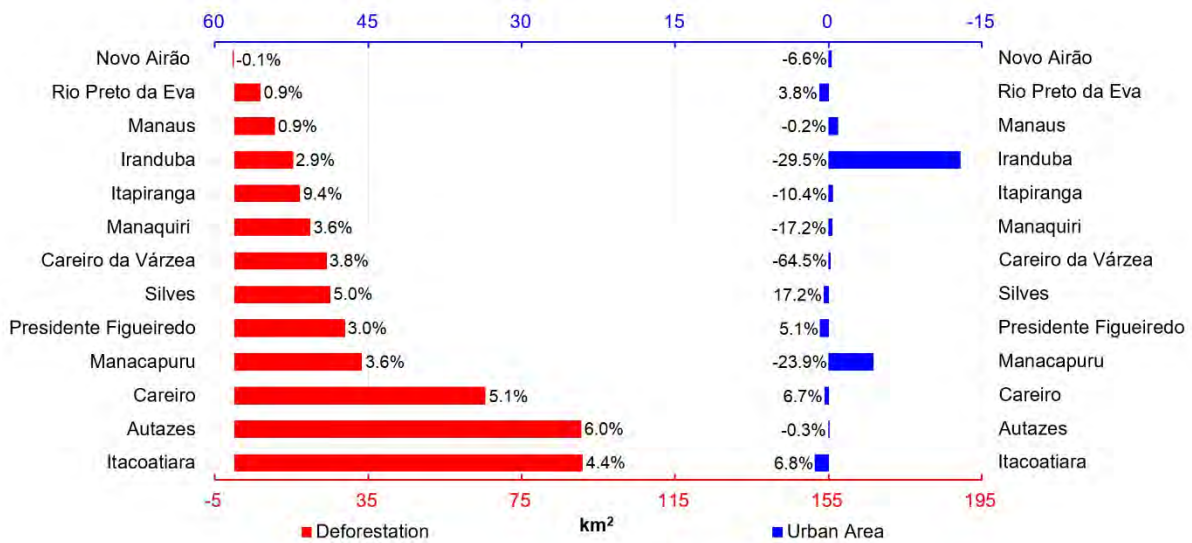


Fig. 6. Difference between the simulated and observed maps of the MMR municipalities for the year 2017. The left side (red bars) represents the deforestation class (km^2), and the right side (blue bars) represents the urban area class (km^2).

266 3.2 Space-time dynamics of deforestation and urban expansion

267

268 Figure 7 illustrates the change in land-use/cover of the MMR for the period from 2017
 269 to 2100 with the urban area of Manaus located in the center of the domain. The expansion of
 270 urban areas (in yellow) and the increases in deforested area (in red) along state and federal
 271 highways are evident. The magnitudes of growth in deforestation and in the urban areas of
 272 the municipalities of Manaus, Itanduba, and Manacapuru also stand out. In the case of
 273 deforestation, the expansion is more accentuated to the south of Manaus, in the region with
 274 the municipalities of Careiro da Várzea, Careiro, and Manaquiri (Figures 7a–d). As of 2050,
 275 the municipalities of Itanduba and Manacapuru display an increase in their deforested area
 276 and a slight increase in their urban areas, especially in the last decades of the 21st century.
 277 The municipalities to the south and southeast of Manaus show a significant expansion of their
 278 deforested areas between 2050 and 2070 (Figures 7e–g). Towards the end of the 21st century,
 279 the urban expansion of the city of Manaus to the north is observed, along the BR-174 and
 280 AM-010 highways. In addition, the preservation of the protection area can be noted
 281 throughout the MMR, as in the case of the Adolpho Ducke Forest Reserve (ADR) in Manaus
 282 (Figures 7h–j).

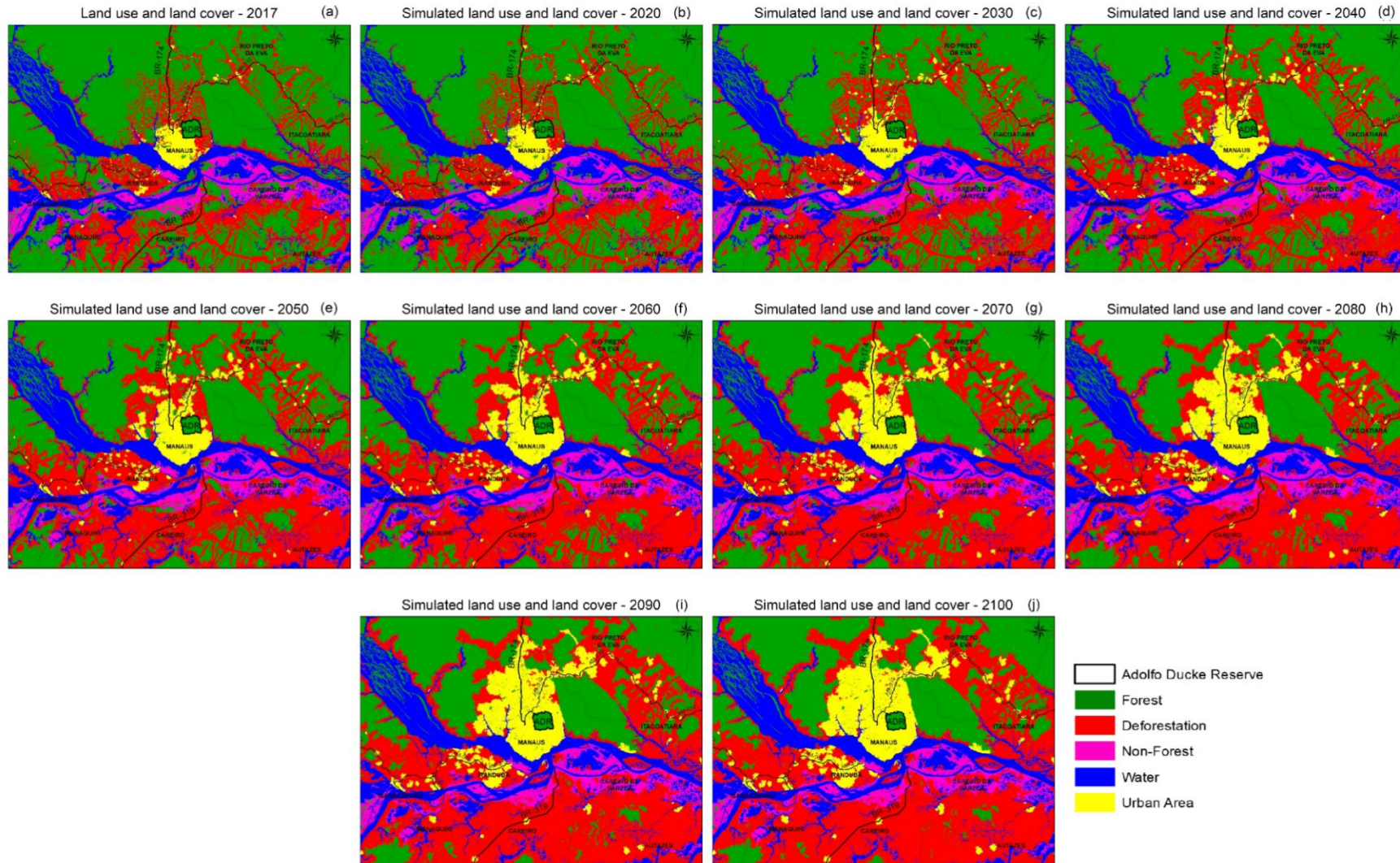


Fig. 7. Spatial evolution of the MMR land-use/cover, for the period from 2017 to 2100, with the urban area of Manaus in the center.

262

263 The data from the simulated land-use/land-cover maps of the MMR for the period from
 264 2017 to 2100 are provided in Table 3. By 2100, the MMR endures an 18% reduction in forest
 265 cover, corresponding to 18,200 km² compared to 2017. The deforested area increases,
 266 approximately, 137% (about 15,300 km²) in relation to 2017 and urban area 555% (3000 km²)
 267 for the same period.

268

Table 3. Temporal evolution of the MMR land use/cover for the period from 2017 to 2100.

Area (km ²)										
Class	2017	2020	2030	2040	2050	2060	2070	2080	2090	2100
Forest	99,115.5	98,259.3	95,539.8	93,009.6	90,649.0	88,441.2	86,371.5	84,427.2	82,596.8	80,870.6
Deforestatio	11,227.8	12,016.0	14,482.2	16,721.4	18,758.1	20,613.0	22,304.9	23,849.6	25,261.6	26,553.4
Urban	525.7	593.6	846.9	1,137.9	1,461.9	1,814.7	2,192.6	2,592.2	3,010.5	3,445.0

269

270 By 2100, all MMR municipalities would have reduced their forest area. The municipalities
 271 Careiro da Várzea, Itacoatiara, Iranduba, and Autazes display percentage forest losses above
 272 50% by the end of the century. The municipalities that presented the greatest reduction of forest
 273 cover are: Itacoatiara (59.1% or 2695.5 km²), Autazes (52.8% or 2545.0 km²), Presidente
 274 Figueiredo (11.5% or 2433.2 km²), and Manaus (27.1% or 2299.9 km²). The forest area in the
 275 municipality of Novo Airão experiences the least impacted due to deforestation by 2100 (1.2%
 276 or 433.8 km²) (see Supplementary Material, Figure S-2).

277 The absolute growth in km² for the deforestation area (red bars) and urban area (blue bars)
 278 of the MMR municipalities and their respective relative values for the period 2017–2100 are
 279 depicted in Figure 8, and the growth values of deforestation and urban area spatially distributed
 280 in the municipalities are illustrated in Figure 9.

281 In 2100, the municipalities of Novo Airão, Presidente Figueiredo, and Itapiranga present an
 282 increase greater than 200% in deforested area, compared to 2017, with Novo Airão being the
 283 municipality with the highest rate of deforestation growth in percentage terms. In terms of
 284 deforested area, Itacoatiara, Autazes, and Presidente Figueiredo are the municipalities that
 285 exhibit increased deforestation above 2000 km² by 2100 (Figure 9a).

286 All municipalities analyzed would increase their urban area by the end of the 21st century
 287 by over 1000% compared to 2017, with the exception of Manaus and Manaquiri (Figure 8). The
 288 municipalities of Manaus, Rio Preto da Eva, Iranduba, and Presidente Figueiredo experience the
 289 greatest growth in urban area in terms of area (> 200 km²) by 2100. Careiro da Várzea is the
 290 municipality that experiences the lowest urban growth (less than 1 km²) (Figure 9b).

291

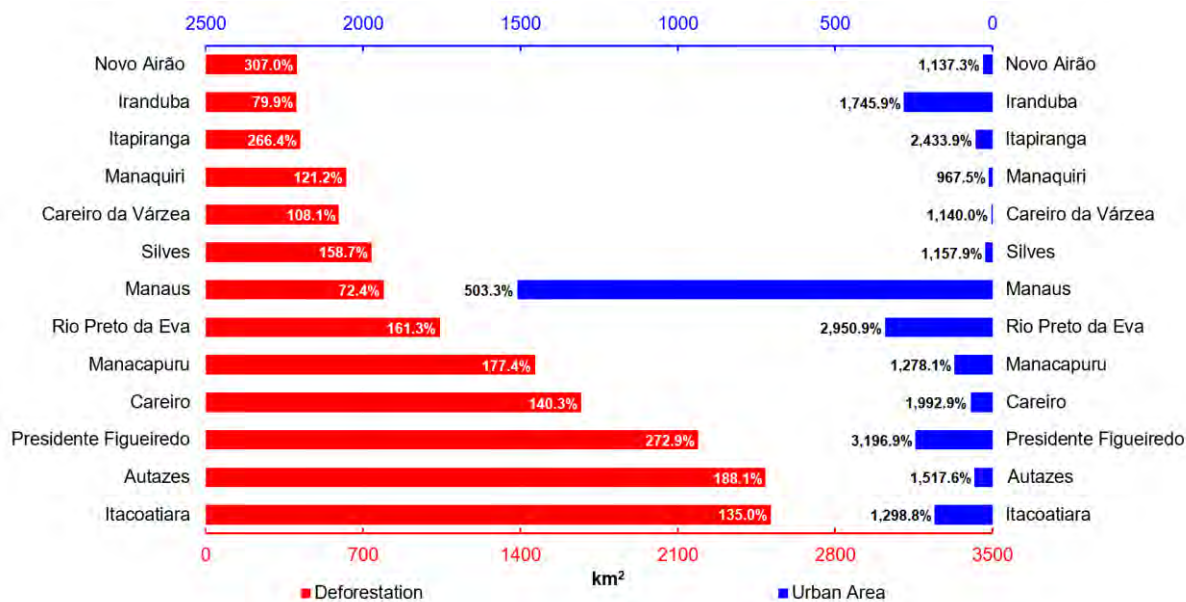


Fig. 8. Growth of the deforestation area and urban area of the MMR municipalities from 2017 to 2100. Deforestation (km²) is represented by the red bars (left side) and the lower axis, while the urban area (km²) is represented by the blue bars (right side) and the upper axis.

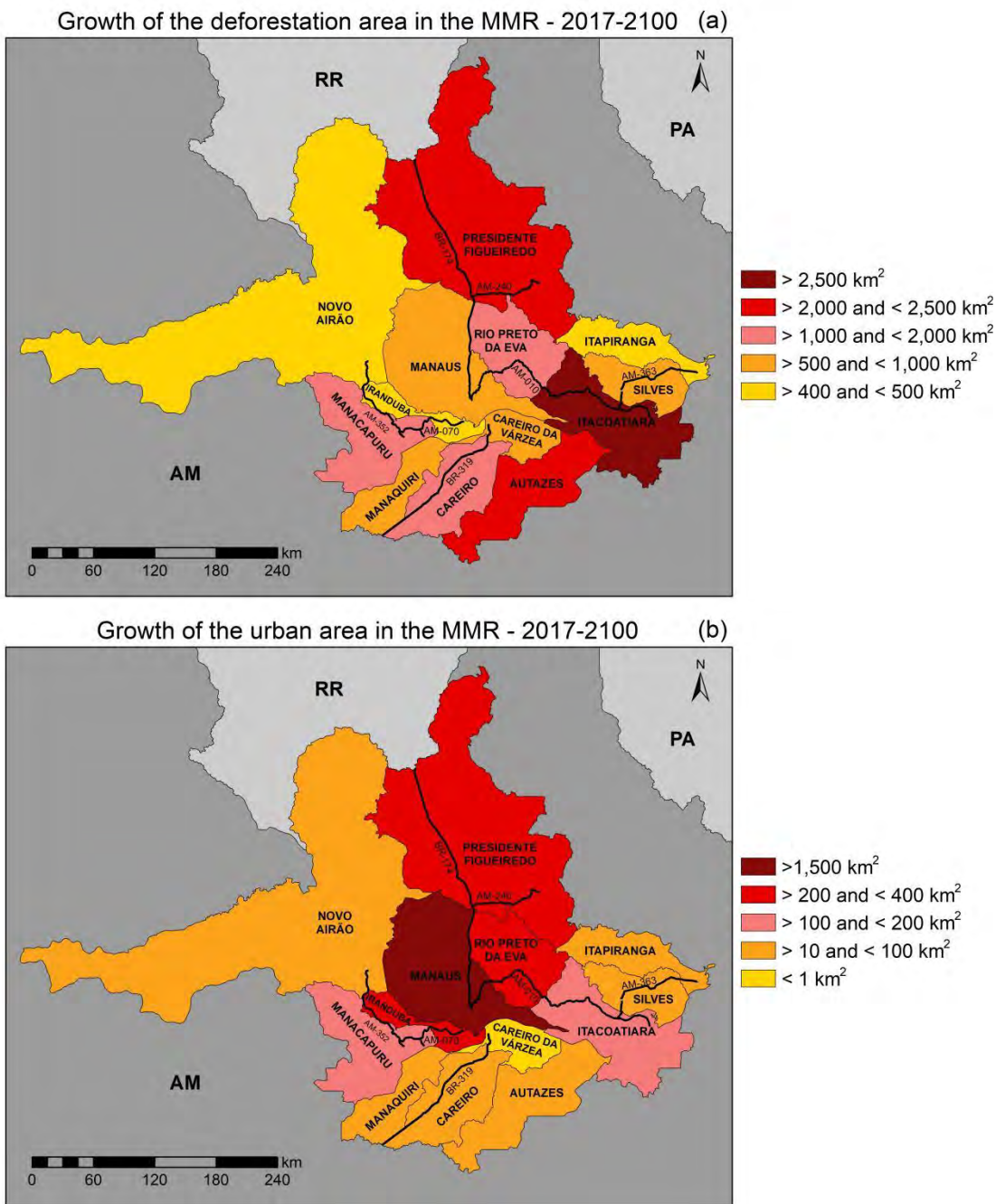


Fig. 9. Spatial distribution of growth in the deforestation area (a) and urban area (b) of the MMR municipalities from 2017 to 2100..

292

293 **4. Discussion**

294 The minimum similarity results obtained are within the validation range found in other
295 studies conducted with Dinamica EGO software as presented in Supplementary Material, Table
296 S-1. The window for which the similarity reached 50% is presented for each study.

297 The large variations in deforestation rates in the Amazon must be considered
298 (Supplementary Material, Figure S-2). The highest peak of deforestation in the Amazon region
299 occurred in 2004, but rates decreased dramatically after that year. In the study area, the rate
300 decreased slightly, but for some municipalities 2008 had one of the highest deforestation rates.
301 The calibration included this period of high deforestation rates for the study area. The lowest
302 point of deforestation for the Legal Amazon occurred in 2012. The study area also experienced
303 one of the lowest deforestation rates in 2012, followed by a fall in the rate for many
304 municipalities in 2013, with trend of increasing rates in the following years.

305 The validation covers the period from 2012 to 2017. From 2018 onwards, a strong trend of
306 increasing deforestation in the Amazon has been observed, with different rates than in the mid-
307 2000s. Waves of deforestation are common trends, as deforestation rates are subject to several
308 factors, including economic cycles, election cycles (both regional and local), environmental
309 protection policies, and changes in infrastructure (such as the construction of a bridge). In this
310 study, the period considers the influence of the Rio Negro Bridge (construction started in 2007)
311 and the creation of the MMR (2007) as a way of including two important facts that may
312 influence the projection of deforestation in the coming years.

313

314 The percentage difference in model validation between the observed map and the 2017
315 simulated map (see Table 4) for the deforestation class obtained in this study is similar to those
316 found in other studies in the Amazon, which were 4.7% (Yanai et al., 2012), 5.3% (Barni et al.,
317 2015), 0.9% (Roriz et al., 2017), and 7.9% (Ramos et al., 2018). No other studies have modeled
318 urban growth for the Amazon region to compare with our result. The percentage differences for
319 the deforestation class and for the urban area class for the year 2017 may be mostly due to the
320 differences in the transition rates of the municipalities used in the calibration and validation (see
321 Supplementary Material, Table S-2 and Figure S-4). The greatest differences between the results
322 in the observed and simulated maps were for the municipalities of Iranduba and Manacapuru,
323 principally in relation to the expansion of the urban area. The simulated amounts of urban growth
324 for Iranduba and Manacapuru are underestimated by -29.5 and -23.9%, respectively. These
325 values represent the largest underestimations in absolute area found in the validation, which were
326 12.9 km² for Iranduba and 4.4 km² for Manacapuru. We chose to employ two different periods
327 for calibration and validation to lessen the spurious effects of using the same transition rates in
328 these two steps. Despite the differences for these two specific municipalities, the result of the
329 validation for the study area was generally satisfactory. However, for the municipalities of
330 Iranduba and Manacapuru, the results for 2100, especially in the case of urban growth, could be
331 considered conservative.

332

333 The spatial model of deforestation and urban expansion used in the present study showed
334 increased loss of forest cover due to the conversion of forest to deforestation and an increase in
335 urban areas due to the advance of deforestation around these urban areas. The construction of the
336 Rio Negro Bridge had an accelerating effect on the dynamics of land-use and cover change for

337 the municipalities that were connected to Manaus by the bridge. Our study incorporated the
338 period of planning and the start of construction of the Rio Negro Bridge from 2007 to 2010 and
339 captured the movement related to land speculation in the region. In the study by Ramos et al.
340 (2018), the scenario simulated with the bridge considered the period from 2008 to 2010 and in
341 our study, the period considered was from 2004 to 2010. Thus, our model considers the
342 deforestation pattern related to the bridge effect. For the transition from deforestation to an urban
343 area, the MMR municipalities showed similar urban growth rates, with the exception of the
344 municipality of Manaus (see Supplementary Material, Figure S-3d).

345
346 The Rio Negro Bridge, inaugurated in 2011, and the good condition of the initial stretch of
347 Highway BR-319 located in the municipalities of Careiro da Várzea and Careiro, demonstrated
348 the influence of road access in increasing deforestation and, subsequently, urban growth. This
349 effect of road access on deforestation has also been observed in other studies in the Amazon,
350 including Dickinson (1989), Soares-Filho et al. (2004), Fearnside (2006), Fearnside et al. (2009),
351 Yanai et al. (2012), Barber et al. (2014), Barni et al. (2015), and Ramos et al. (2018). Another
352 important aspect is the effect of protected areas in preventing deforestation, contributing to the
353 conservation of the forest. Novo Airão would have the smallest area deforested by the end of the
354 century (Figure 8, see Supplementary Material, Figure S-1) because this municipality has a vast
355 area of forest occupied by conservation units and is also far from the main highways (BR-174
356 and BR-319) (Figure 1). Yanai et al. (2012) showed how protected areas are important for
357 curbing deforestation and the emergence of secondary roads, although protected do not entirely
358 prevent deforestation (see Supplementary Material, Table S-4).

359
360 Our results also show urban expansion of the MMR near the already-urbanized areas, as
361 was found in the State of São Paulo a study by Almeida et al. (2008). These authors simulated
362 changes in intra-urban land use in a medium-sized city and showed that new residential and
363 industrial subdivisions tend to appear around areas where these types of subdivisions already
364 exist and in areas with good accessibility and/or that are near the main roads. Service corridors
365 usually run along major roads and close to larger residential and commercial areas, and areas for
366 subdivisions follow the same growth logic as industrial zones.

367
368 Despite its small urban area, the municipality of Careiro da Várzea has a high percentage
369 of urban growth at the end of the century (see Figure 9). Although the municipality of Manaus
370 had the highest rate of urban growth in the calibration period (2004-2010), in the validation
371 period (2012-2017), and in the entire period analyzed (2004-2017) – 1% per year
372 (Supplementary Material, Table S-2) and had the largest urban area at the end of the century
373 (1508 km²) – Manaus demonstrates the lowest urban growth during the simulation (503.3%).
374 This result may be because the municipality of Manaus contains extensive conservation units and
375 special areas (see Figures 1 and 3) that inhibit deforestation and consequently urban growth. This
376 reinforces the importance of protected areas in forest conservation (Yanai et al., 2012). In
377 addition, Manaus has a more consolidated urbanization process, while the other the MMR
378 municipalities are in the initial process of expanding their urban area.

379
380 The influence of the road system on the growth of deforestation in the MMR is obvious.
381 For example, the municipality of Presidente Figueiredo has extensive conservation areas (see
382 Figure 1) and the second lowest rate of deforestation transition (Supplementary Material, Table

383 S-2), but the simulation showed extensive deforested by 2100 as compared to the area deforested
 384 by 2017. Highway BR-174, which connects Manaus with the State of Roraima, passes through a
 385 large part of this municipality. Presidente Figueiredo is also crossed by Highway AM-240. The
 386 southeastern portion of the MMR undergoes a greater expansion of deforestation (see Figure 9a
 387 and Supplementary Material, Figure S-2), which can be explained by the conditions of the
 388 highways in the study perimeter (BR-174 and AM-010).

389
 390 The urban growth of the MMR seems to be strongly associated with pre-existing urban
 391 areas as well as with accessible transport routes, as presented by Almeida et al. (2008). The
 392 influence of the AM-070 and the Rio Negro Bridge for the expansion of the urban area of
 393 Iranduba and Manacapuru stand out. The municipalities interconnected by Highways BR-174,
 394 AM-010, and AM-070 had greater expansion of their urban areas than other municipalities (see
 395 Figure 9b). This confirms the influence of transport infrastructure on the increase in peri-urban
 396 deforestation (Ramos et al., 2018) and, consequently, on urban expansion.

397
 398 Our results can be considered conservative, since there was still no paving of BR-319 and
 399 duplication of AM-010, which are expected to start in the coming years. This could accelerate
 400 the migration of deforestation to the Manaus area from the “arc of deforestation” (the heavily
 401 deforested strip along the southern and eastern edges of the Brazilian Amazon), as well as
 402 increase urban expansion due to population growth, such as the invasion of land for subdivisions
 403 on the outskirts of Manaus and neighboring municipalities.

404
 405 Our results can assist public and private entities responsible for urban and environmental
 406 planning in the Amazon region and help in decision-making on urban planning and expansion of
 407 the road network. Future work could include socio-economic variables in the modeling, such as
 408 expansion of tax exemptions in the Manaus Free Trade Zone for the entire MMR (Laws No.
 409 6951/2017 and No. 2633/2011), demographics, real estate speculation, per-capita income, the
 410 future market for agricultural commodities, and cattle ranching.

412 5. Conclusions

413 Deforestation projected to 2100 in the Manaus Metropolitan Region (MMR) is
 414 concentrated along the main and secondary roads. The simulated scenario indicates that, if
 415 deforestation rates persist, most the municipalities in the MMR would experience an increase of
 416 more than 100% in their deforested areas by the end of this century. Some MMR municipalities
 417 would have urban areas expand by over 500% by 2100. Thus, urbanization in the MMR may also
 418 represent a new “frontier” that will contribute to exacerbate the loss of Amazonian forests by
 419 increasing pressure for new deforested areas.

420 References

Allen, A. (2003). Environmental planning and management of the peri-urban interface: perspectives on an emerging field. *Environment and Urbanization*, 15(1), 135-148. <https://doi.org/10.1177/095624780301500103>.

Almeida, C., Batty, M., Monteiro, A., Câmara, G., Soares-Filho, B. S., Cerqueira, G., & Pennachin, C. L. (2003). Stochastic cellular automata modeling of urban land use dynamics:

empirical development and estimation. *Computers, Environment and Urban Systems*, 27(5), 481-509. [https://doi.org/10.1016/S0198-9715\(02\)00042-X](https://doi.org/10.1016/S0198-9715(02)00042-X).

Almeida, C. M., Gleriani, J. M., Castejon, E. F., & Soares-Filho, B. S. (2008). Neural networks and cellular automata for modeling intra-urban land use dynamics. *International Journal of Geographical Information Science*, 22(9), 943-963. <https://doi.org/10.1080/13658810701731168>.

Barbieri, A. F., & Carr, D. L. (2005). Gender-specific out-migration, deforestation and urbanization in the Ecuadorian Amazon. *Global and Planetary Change*, 47(2), 99–110. <https://doi.org/10.1016/j.gloplacha.2004.10.005>.

Barber, C. P., Cochrane, M. A., Souza Junior, C. M., & Laurance, W. F. (2014). Roads, deforestation, and the mitigating effect of protected areas in the Amazon. *Biological Conservation*, 77, 203-209. <https://doi.org/10.1016/j.biocon.2014.07.004>.

Barni, P. E., Fearnside, P. M., & Graça, P. M. L. A. (2015). Simulating Deforestation and Carbon Loss in Amazonia: Impacts in Brazil's Roraima State from Reconstructing Highway BR-319 (Manaus-Porto Velho). *Environmental Management*, 55(2), 259-278. <https://doi.org/10.1007/s00267-014-0408-6>.

Becker, B. K. (2001). Revisão das Políticas de Ocupação da Amazônia: é possível identificar modelos para projetar cenários? *Parcerias Estratégicas*, 6(12), 135–159. Retrieved from – http://seer.cgee.org.br/index.php/parcerias_estrategicas/article/viewFile/178/172.

Becker, B. K. (2005). Geopolítica da Amazônia. *Estudos Avançados*, 19(53), 71-86. <https://doi.org/10.1590/S0103-40142005000100005>.

Bonham-Carter, G. F. (1994). *Geographic Information Systems for Geoscientists: Modelling with GIS*. Pergamon. Retrieved from – <https://www.sciencedirect.com/book/9780080418674/geographic-information-systems-for-geoscientists>.

Bonham-Carter, G., Agterberg, F. P., & Wright, D. (1989). Weights of evidence modelling: a new approach to mapping mineral potential. *Statistical Applications in The Earth Sciences*, 89(9), 171-183. <https://doi.org/10.4095/128059>.

Brando, P. M., Balch, J. K., Nepstad, D. C., Morton, D. C., Putz, F. E., Coe, M. T., Silvério, D., Macedo, M. N., Davidson, E. A., Nóbrega, C. C., Alencar, A., & Soares-Filho, B. S. (2014). Abrupt increases in Amazonian tree mortality due to drought–fire interactions. *PNAS*, 111(17), 6347-6352. <https://doi.org/10.1073/pnas.1305499111>.

Brando, P. M., Soares-Filho, B., Rodrigues, L., Assuncao, A., Morton, D., Tuchsneider, D., Fernandes, E. C. M., Macedo, M. N., Oliveira, U., & Coe, M. T. (2020). The gathering firestorm in southern Amazonia. *Science Advances*, 6(2), eaay1632. <https://doi.org/10.1126/sciadv.aay1632>.

Costa, F. G., Caixeta-Filho, J. V., & Arima, E. (2019). Influência do transporte no uso da terra: o potencial de viabilização da produção de soja na Amazônia Legal devido ao desenvolvimento da infra-estrutura de transportes. *Revista de Economia e Sociologia Rural*, 39(2), 27-50. Retrieved from <http://www.resr.periodikos.com.br/article/5d8b9ece0e8825613df2a2f5/pdf/resr-39-2-27.pdf>.

Costa, J., Rodrigues, L., Mendonça, M., Melo, M., & Liberato, M. (2020). Diagnóstico ambiental do baixo curso do Igarapé do Gigante (Amazonas – Brasil). *Ciência e Natura*, 42, e97. doi:<https://doi.org/10.5902/2179460X40562>.

Costa, W. M. (2000). *O Estado e as Políticas Territoriais no Brasil*. Contexto.

de Souza, D.O., & dos Santos Alvalá, R. C. (2014). Observational evidence of the urban heat island of Manaus City, Brazil. *Meteorological Applications*, 21, 186-193. <https://doi.org/10.1002/met.1340>.

Dickinson, R. E. (1989). Modeling the effects of Amazonian deforestation on regional surface climate: A review. *Agricultural and Forest Meteorology*, 47, 339-347. [https://doi.org/10.1016/0168-1923\(89\)90104-4](https://doi.org/10.1016/0168-1923(89)90104-4).

Faria, B. L., Brando, P. M., Macedo, M. N., Panday, P. K., Soares-Filho, B. S., & Coe, M. T. (2017). Current and future patterns of fire-induced forest degradation in Amazonia. *Environmental Research Letters*, 12(9), 095005. <https://doi.org/10.1088/1748-9326/aa69ce>.

Fearnside, P. M. (2006). Desmatamento na Amazônia - dinâmica, impactos e controle. *Acta Amazonica*, 36(3), 395–400. <https://doi.org/10.1590/S0044-59672006000300018>.

Fearnside, P. M., Graça, P. M. L. A., Keizer, E. W. H., Maldonado, F. D., Barbosa, R. I., & Nogueira, E. M. (2009). Modelagem de desmatamento e emissões de gases de efeito estufa na região sob influência da Rodovia Manaus-Porto Velho (BR-319). *Revista Brasileira de Meteorologia*, 24(2), 208–233. <https://doi.org/10.1590/S0102-77862009000200009>.

Fonseca, P. A. M., Hacon, S. S., Reis, V. L., Costa, D., & Brown, I. F. (2016). Using satellite data to study the relationship between rainfall and diarrheal diseases in a Southwestern Amazon basin. *Ciência & Saúde Coletiva*, 21(3), 731-742. <https://doi.org/10.1590/1413-81232015213.20162015>.

Góes Filho, S. S. (2015). *Navegantes, bandeirantes, diplomatas: um ensaio sobre a formação das fronteiras do Brasil*. Funag.

Gonçalves, D. A. (2008). *Modelagem dinâmica espacial para a geração de cenários de ocupação na Amazônia sul-ocidental*. Dissertação de Mestrado em Ciências. Instituto Tecnológico de Aeronáutica – ITA – São José dos Campos, SP, Brazil.

Google Earth Pro v7.3.2. (June 29, 2018). Manaus, Brazil. 2° 57' 32"S, 60° 02' 57"W, Eye alt 423 m. Borders and labels; places layers. Landsat/Copernicus. (Accessed October 23, 2018).

Guedes, G. R., Costa, S. M., & Brondizio, E. (2009). Revisiting the hierarchy of urban areas in the Brazilian Amazon: a multilevel approach. *Population and Environment*, 30(4-5), 159–192. <https://doi.org/10.1007/s11111-009-0083-3>.

Guerra, J. B., Mura, J. C., & Freitas, C. D. C. (2010). Discriminação de incrementos de desflorestamento na Amazônia com dados SAR R99B em banda L. *Acta Amazonica*, 40(3), 557-565. <https://doi.org/10.1590/S0044-59672010000300015>.

Hagen, A. (2003). Fuzzy set approach to assessing similarity of categorical maps. *International Journal of Geographical Information Science*, 17(3), 235-249. <https://doi.org/10.1080/13658810210157822>.

IBGE. (2010). Brazilian Institute of Geography and Statistics. In *Sinopse do censo demográfico 2010*. Retrieved January 27, 2018 from <https://censo2010.ibge.gov.br/sinopse/index.php?uf=13&dados=21>.

IBGE. (2019a). Brazilian Institute of Geography and Statistics. In *Regiões Metropolitanas, Aglomerações Urbanas e Regiões Integradas de Desenvolvimento*. Retrieved December 15, 2019 from <https://bit.ly/6WBW>.

IBGE. (2019b). Brazilian Institute of Geography and Statistics. In *Cidades*. Retrieved December 15, 2019 from <https://cidades.ibge.gov.br/>.

Ignotti, E., Valente, J. G., Longo, K. M., Freitas, S. R., Hacon, D. D., & Netto, P. A. (2010). Impact on human health of particulate matter emitted from burnings in the Brazilian Amazon region. *Revista de Saúde Pública*, 44(1), 121-130. <https://doi.org/10.1590/S0034-89102010000100013>.

Imbiriba, E. N. B., Silva Neto, A. L. D., Souza, W. V. D., Pedrosa, V., Cunha, M. D. G., & Garnelo, L. (2009). Social inequality, urban growth and leprosy in Manaus: a spatial approach. *Revista de Saude Publica*, 43, 656-665. <https://doi.org/10.1590/S0034-89102009005000046>.

INPE. (2017). National Institute of Space Research. Centro Regionais da Amazônia. TerraClass. In *Projeto TerraClass 2014*. Retrieved November 10, 2017 from <http://terraBrasilis.dpi.inpe.br/downloads/>.

Kalnay, E., & Cai, M. (2003) Impact of urbanization and land-use change on climate. *Nature*, 423, 528-531. <https://doi.org/10.1038/nature01675>.

Kuwahara, N., Neto, J. C. L., & Abensur, T. C. (2012). Modelagem de previsão de navegabilidade em rios da Amazônia: ferramenta web de suporte aos usuários do transporte aquaviário. *Journal of Transport Literature*, 6(3), 60–89. <https://doi.org/10.1590/S2238-10312012000300005>.

MapBiomias Project. (2018). In *Coleção 3 da Série Anual de Mapas de Cobertura e Uso de Solo do Brasil*. Retrieved October 31, 2018 from <http://mapbiomas.org>.

MMA. (2019). Ministry of the Environment. In *Amazônia*. Retrieved June 9, 2019 from <https://www.mma.gov.br/biomias/amaz%C3%B4nia.html>.

Moreira, F., Fontes, I., Dias, S., Batista e Silva, J., & Loupa-Ramos, I. (2016). Contrasting static versus dynamics-based typologies of land cover patterns in the Lisbon metropolitan area: towards a better understanding of peri-urban areas. *Applied Geography*, 75, 49–59. <https://doi.org/10.1016/j.apgeog.2016.08.004>.

Osis, R., Laurent, F., & Pocard-Chapuis, R. (2019). Spatial determinants and future land use scenarios of Paragominas municipality, an old agricultural frontier in Amazonia. *Journal of Land Use Science*, 14(3), 258-279. <https://doi.org/10.1080/1747423X.2019.1643422>

Paegelow, M., Camacho Olmedo M. T. & Mas J. F. (2018) *Techniques for the Validation of LUCC Modeling Outputs*. In: Camacho Olmedo M., Paegelow M., Mas J. F., Escobar F. (eds) *Geomatic Approaches for Modeling Land Change Scenarios*. Lecture Notes in Geoinformation and Cartography. Springer. https://doi.org/10.1007/978-3-319-60801-3_4.

Paiva, A. C. E., Nascimento, N., Rodriguez, D. A., Tomasella, J., Carriello, F., & Rezende, F. S. (2020). Urban expansion and its impact on water security: The case of the Paraíba do Sul River Basin, São Paulo, Brazil. *Science of The Total Environment*, 720, 137509. <https://doi.org/10.1016/j.scitotenv.2020.137509>.

Pavão, M. (2017). *Modelagem e análise de mudanças do uso e cobertura da terra no entorno de áreas protegidas: o caso do Parque Estadual da Cantareira* (Doctoral thesis in physical geography). Universidade de São Paulo, Departamento de Geografia, São Paulo, SP, Brazil.

Pontius Jr., R. G., Boersma, W., Castella, J. C., Clarke, K. C., de Nijs, T., Dietzel, C., Duan, Z., Fotsing, E., Goldstein, N., Kok, K., Koomen, E., Lippitt, C. D., McConnell, W., Sood, A. M., Pijanowski, B., Pithadia, S., Sweeney, S., Ngoc Trung, T., Veldkamp, A., & Verburg, P. H. (2008). Comparing the input, output, and validation maps for several models of land change. *The Annals of Regional Science*, 42, 11–37. <https://doi.org/10.1007/s00168-007-0138-2>.

Powell, R. L., Roberts, D. A., Dennison, P. E., & Hess, L. L. (2007). Sub-pixel mapping of urban land cover using multiple endmember spectral mixture analysis: Manaus, Brazil. *Remote Sensing of Environment*, 106(2), 253-267. <https://doi.org/10.1016/j.rse.2006.09.005>.

PRODES. (2019). National Institute of Space Research. (INPE) Coordenação Geral de Observação da Terra. Programa de Monitoramento da Amazônia e demais biomas. In *Desmatamento – Amazônia Legal – PRODES*. Retrieved July 5, 2018 from <http://terrabilis.dpi.inpe.br/downloads/>.

Ramos, C. J. P., Graça, P. M. L. A. G., & Fearnside, P. M. (2018). Deforestation Dynamics on an Amazonian Peri-Urban Frontier: Simulating the Influence of the Rio Negro Bridge in Manaus, Brazil. *Environmental Management*, *62*(6), 1134-1149. <https://doi.org/10.1007/s00267-018-1097-3>.

Resende, T. V. F. (2006). *A conquista e a ocupação da Amazônia brasileira no período colonial: a definição das fronteiras* (Doctoral thesis in history). Universidade de São Paulo, Departamento de História Econômica, São Paulo, SP, Brazil.

Ritchie, H., & Roser, M. (2018). Urbanization. Our world in data. Retrieved June 12, 2019 from <https://ourworldindata.org/urbanization>.

Roriz, P. A. C., Yanai, A. M., & Fearnside, P. M. (2017). Deforestation and carbon loss in Southwest Amazonia: impact of Brazil's revised forest code. *Environmental Management*, *60*(3), 367-382. <https://doi.org/10.1007/s00267-017-0879-3>.

Sant'Anna, J. A. (1998). Rede básica de transporte na Amazônia. Retrieved April 12, 2018 from http://www.ipea.gov.br/agencia/images/stories/PDFs/Tds/td_0562.pdf.

Schor, T., & Oliveira, J. A. (2011). Reflexões metodológicas sobre o estudo da rede urbana no Amazonas e perspectivas para a análise das cidades na Amazônia Brasileira. *Acta Geográfica, Ed. Esp. Cidades na Amazônia Brasileira*, 15-30. <https://doi.org/10.5654/acta.v5i11.539>.

Silvestrini, R. A., Soares-Filho, B. S., Nepstad, D., Coe, M., Rodrigues, H., & Assunção, R. (2011). Simulating fire regimes in the Amazon in response to climate change and deforestation. *Ecological Applications*, *21*, 1573-1590. <https://doi.org/10.1890/10-0827.1>

Sirakoulis, G. C., Karafyllidis, I., & Thanailakis, A. (2000). A cellular automaton model for the effects of population movement and vaccination on epidemic propagation. *Ecological Modelling*, *133*, 209-223. [https://doi.org/10.1016/S0304-3800\(00\)00294-5](https://doi.org/10.1016/S0304-3800(00)00294-5).

Soares-Filho, B. S., Alencar, A., Nepstad, D., Cerqueira, G., Diaz, M. C. V., Rivero, S., Solórzanos, L., & Voll, E. (2004). Simulating the response of land-cover changes to road paving and governance along a major Amazon highway: The Santarém-Cuiabá corridor. *Global Change Biology*, *10*(5), 745-764. <https://doi.org/10.1111/j.1529-8817.2003.00769.x>.

Soares-Filho, B. S., Cerqueira, G. C., & Pennachin, C. L. (2002). DINAMICA — a stochastic cellular automata model designed to simulate the landscape dynamics in an Amazonian colonization frontier. *Ecological Modelling*, *154*(3), 217-235. [https://doi.org/10.1016/S0304-3800\(02\)00059-5](https://doi.org/10.1016/S0304-3800(02)00059-5).

Soares-Filho, B. S., Nepstad, D., Curran, L., Voll, E., Cerqueira, G., Garcia, R. A., Ramos, C. A., McDonald, A., Lefebvre, P., & Schlesinger, P. (2006). Modeling Conservation in the Amazon Basin. *Nature*, *440*, 520-523. <https://doi.org/10.1038/nature04389>.

- Soares-Filho, B. S., Rodrigues, H. O., & Costa, W. L. (2009). *Modeling Environmental Dynamics with Dinamica EGO: Guidebook*. Retrieved October 10, 2017 from <https://csr.ufmg.br/dinamica/dokuwiki/doku.php?id=tutorial:start>.
- Soares-Filho, B. S., Silvestrini, R., Nepstad, D., Brando, P., Rodrigues, H., Alencar, A., Coe, M., Locks, C., Lima, L., Hissa, L., & Stickler, C. (2012). Forest fragmentation, climate change and understory fire regimes on the Amazonian landscapes of the Xingu headwaters. *Landscape Ecology*, 27, 585–598. <https://doi.org/10.1007/s10980-012-9723-6>.
- Soares-Filho, B. (2015). In *Validation*. Retrieved June 6, 2018 from <https://csr.ufmg.br/dinamica/validation/>.
- Sousa, I. S. (2015). *A ponte Rio Negro e a reestruturação do espaço na Região Metropolitana de Manaus: Um olhar a partir de Iranduba e Manacapuru* [The Rio Negro Bridge and the restructuring of space in the Manaus Metropolitan Region: A view from Iranduba and Manacapuru]. Editora Reggo and UEA Edições, Manaus, AM, Brazil, 176 pp.
- Souza, D. O. de, dos Santos Alvalá, R. C., & do Nascimento, M. G. (2016). Urbanization effects on the microclimate of Manaus: A modeling study. *Atmospheric Research*, 167, 237-248. <https://doi.org/10.1016/j.atmosres.2015.08.016>.
- Thapa, R. B., & Murayama, Y. (2011a). *Spatiotemporal Patterns of Urbanization: Mapping, Measurement, and Analysis*. In: Murayama Y., Thapa R. (eds) *Spatial Analysis and Modeling in Geographical Transformation Process*. GeoJournal Library, v. 100. Springer, Dordrecht, The Netherlands.
- Thapa, R. B. & Murayama, Y. (2011b). Urban growth modeling of Kathmandu metropolitan region, Nepal. *Computers, Environment and Urban Systems*, 35, 25–34. <https://doi.org/10.1016/j.compenvurbsys.2010.07.005>.
- Tucci, C. E. M. (2008). Águas urbanas. *Estudos Avançados*, 22(63), 97-112. Retrieved October 18, 2020 from <https://www.revistas.usp.br/eav/article/view/10295>.
- United Nations. (2019). *Department of Economic and Social Affairs, Population Division World Urbanization Prospects: The 2018 Revision*. Retrieved April 19, 2019 from <https://population.un.org/wup/>.
- Vitel, C. S. M. N., Fearnside, P. M., & Graça, P. M. L. A. (2009). Análise da inibição do desmatamento pelas áreas protegidas na parte Sudoeste do Arco de desmatamento. In: Anais XIV Simpósio Brasileiro de Sensoriamento Remoto, Natal, Rio Grande do Norte: Instituto Nacional de Pesquisas Espaciais, São José dos Campos, SP, Brazil. pp. 6377-6384. <http://marte.sid.inpe.br/col/dpi.inpe.br/sbsr%4080/2008/11.13.14.42/doc/6377-6384.pdf>
- Walker, W. S., Stickler, C. M., Kellndorfer, J. M., Kirsch, K. M., & Nepstad, D. (2010). Large area classification and mapping of forest and land cover in the Brazilian Amazon: a comparative analysis of ALOS/PALSAR and Landsat data sources. *Journal of Selected Topics in Applied*

Earth Observations and Remote Sensing 3, 594–604.
<https://doi.org/10.1109/JSTARS.2010.2076398>.

Xie, Y. (1996). A generalized model for cellular urban dynamics. *Geographical Analysis*, 28(4), 350-373. <https://doi.org/10.1111/j.1538-4632.1996.tb00940.x>.

Ximenes, A. C., Almeida, C. M., Amaral, S., Escada, M. I. S., & Aguiar, A. P. D. (2008). Modelagem Dinâmica do Desmatamento na Amazônia. *Boletim de Ciências Geodésicas*, 14(3), 370-391. ISSN: 1413-4853. Retrieved April 19, 2019 from <https://www.redalyc.org/articulo.oa?id=393937705005>.

Yanai, A. M., Fearnside, P. M., Graça, P. M. L., A., & Nogueira, E. M. (2012). Avoided deforestation in Brazilian Amazonia: simulating the effect of the Juma Sustainable Development Reserve. *Forest Ecology and Management*, 282, 78-91.
<https://doi.org/10.1016/j.foreco.2012.06.029>.

Yeh, A. G. O., & Li, X. (2006). Errors and uncertainties in urban cellular automata. *Computers, Environment and Urban Systems*, 30(1), 10-28.
<https://doi.org/10.1016/j.compenvurbsys.2004.05.007>.

Young, A. F. (2013) Urban expansion and environmental risk in the São Paulo Metropolitan Area. *Climate Research*, 57, 73–80. <https://doi.org/10.3354/cr01161>.

Figure 1. Study area.	4
Figure 2. Methodology for obtaining the 2017 land-use/cover map. The residual deforestation class corresponds to errors of omission in the PRODES mapping of previous years (Guerra et al., 2010). Deforestation is the deforestation of PRODES without overlapping with the urban area.	7
Figure 3. Static variables used in the model: (a) Elevation, (b) Slope, (c) Conservation units, (d) Settlements and Quilombola Area, (e) Indigenous lands and Special areas, (f) Distance to rivers, (g) Distance to the main highways, (h) Soil, and (i) Vegetation. The distance and elevation variables are expressed in meters while the slope is in degrees.	8
Figure 4. Minimum values of fuzzy similarity with multiple resolution adjustment using the constant decay function. “Window size” is the number of cells (pixels) on each side of the square window area.	14
Figure 5. Expanded detail comparing the observed and simulated land use maps for 2017, with emphasis on the Adolfo Ducke Reserve (ADR) area located in the urban area of Manaus (in the center).	14
Figure 6. Difference between the simulated and observed maps of the MMR municipalities for the year 2017. The left side (red bar) represents the deforestation class, and the right side (blue bar) represents the urban area class.	16
Figure 7. Spatial evolution of the MMR land-use/cover, for the period from 2017 to 2100, with the urban area of Manaus in the center.	18
Figure 8. Growth of the deforestation area and urban area of the MMR municipalities from 2017 to 2100. Deforestation is represented by the red bars (left side) and the lower axis, while the urban area is represented by the blue bars (right side) and the upper axis.	20
Figure 9. Spatial distribution of growth in the deforestation area (a) and urban area (b) of the MMR municipalities from 2017 to 2100.	21
Table 1. Sources of maps prepared as input to the land-use/cover model.	9
Table 2. Land-use/land-cover data for the MMR in 2017, from observed and simulated maps.	15
Table 3 . Temporal evolution of the MMR land use/cover, for the period from 2017 to 2100. ..	19
Appendix 1. The PRODES project.	37
Appendix 2. Attractiveness and friction maps.	37
Appendix 3. The Module Change Matrix function.	37
Table S-1. Similarities achieved in Dinamica EGO models in the Amazon.	38
Table S-2. Values of the initial net rates for deforestation and urban expansion of the MMR for different time intervals between 2004 and 2017.	39
Table S-3. Model configuration for land-use/cover simulation the MMR. The transitions considered are Forest to Deforestation and Deforestation to Urban Area.	40
Table S-4. Deforested area and urban area of protection units, Indigenous lands, and special areas (parks and military areas) for the period from 2020 to 2100 for the MMR.	41
Figure S-1. Percentage rates of forest loss in the municipalities of the MMR from 2017 to 2100.	42
Figure S-2. Map of land use/cover in 2017 and expected change of land use/cover in 2100 for the MMR.	43
Figure S-3. Values of deforestation rates of increase for the Legal Amazon region (yellow bar), the state of Amazonas (blue bar), and the MMR municipalities for the period between 2004 and 2017. Sources: PRODES (2019a); PRODES (2019b); INPE (2017).	44
Figure S-4. Spatial distribution of the difference between deforestation areas and	

urban areas between the observed and simulated 2017 maps for the MMR.	45
References	46

Supplementary Material

Amazon deforestation and urban expansion: simulating future growth in the Manaus Metropolitan Region, Brazil

Appendix 1. The PRODES project

The PRODES project performs satellite monitoring of deforestation in the Brazilian Legal Amazon region by identifying and delimiting deforested areas where there has been complete removal of forest cover (i.e., clear cutting) of at least 6.25 ha. The TerraClass project classifies deforestation into different types of land use/cover, based on the PRODES project, with data for the years 2004, 2008, 2010, 2012, and 2014 (INPE, 2017).

Appendix 2. Attractiveness and friction maps.

Attractiveness and friction maps assist in allocating new secondary roads each year of the simulation. These maps are used in the road-builder module. The road-builder module identifies the lowest-cost route for the construction of new roads, taking into account the level of attractiveness and friction of the simulated region (Soares-Filho et al., 2009). The attractiveness map was built based on a multicriteria analysis assigning weights to areas considered attractive for human activities, such as those close to existing roads, previously deforested areas, and urban areas. Similarly, the combination of protected areas (conservation units, Indigenous lands, Quilombola lands) and special areas such as the Adolpho Ducke Forest Reserve (ADR) and military areas was used to create the friction map, which represents the relative cost of road construction.

Appendix 3. The Module Change Matrix function

The Module Change Matrix function concerns the proportion of status changes in the expander function performed at each transition. Since the cell size is equal to 1 hectare, the simulated patches will have a mean of 5 ha with a range of zero to 10 ha for the transition from forest to deforestation. For the transition from deforestation to urban area, the simulated patches will have a mean of 5 ha without variation in their size. Finally, the Patch Isometry parameter defines the shape of the simulated patches, ranging from 0 to 2. The closer to 2 the more isometric the simulated patches will be (Soares-Filho et al., 2009).

Table S-1. Similarities achieved in Dinamica EGO models in the Amazon.

Resolution	Similarity (%)	Window (pixel) with 50% similarity	Reference
100 m	57	7×7	This Study
250 m	55	7×7	Barni, 2015
250 m	57	5×5	Yanai et al., 2012
120 m	50	11×11	Ramos et al., 2018
100 m	59		Teixeira and Soares-Filho., 2009
100 m	50	11×11	Maeda et al., 2011
30 m	54	5×5	Roriz et al., 2017

Table S-2. Values of the initial net rates for deforestation and urban expansion of the MMR for different time intervals between 2004 and 2017.

Forest-Deforestation transition rates per year						
Municipality	2004-2010	2010-2017	2012-2017	2004-2014	2014-2017	2004-2017
Autazes	0.00956	0.00574	0.00565	0.00875	0.00336	0.00751
Careiro	0.00600	0.00313	0.00303	0.00559	0.00070	0.00446
Careiro da Várzea	0.02508	0.01629	0.01793	0.02314	0.01105	0.02036
Iranduba	0.00997	0.00744	0.00967	0.01062	0.00255	0.00880
Itacoatiara	0.01149	0.00628	0.00728	0.01057	0.00244	0.00870
Itapiranga	0.00162	0.00106	0.00073	0.00165	0.00022	0.00133
Manacapuru	0.00573	0.00360	0.00433	0.00556	0.00139	0.00460
Manaquiri	0.00287	0.00152	0.00155	0.00260	0.00062	0.00214
Manaus	0.00391	0.00288	0.00359	0.00444	0.00038	0.00346
Novo Airão	0.00015	0.00012	0.00015	0.00016	0.00004	0.00013
Presidente Figueiredo	0.00149	0.00126	0.00120	0.00163	0.00053	0.00137
Rio Preto da Eva	0.00383	0.00282	0.00347	0.00407	0.00086	0.00331
Silves	0.00431	0.00237	0.00227	0.00411	0.00045	0.00326
Deforestation-Urban transition rates per year						
Municipality	2004-2010	2010-2017	2012-2017	2004-2014	2014-2017	2004-2017
Autazes	0.00024	0.00024	0.00024	0.00024	0.00030	0.00026
Careiro	0.00038	0.00024	0.00033	0.00033	0.00024	0.00032
Careiro da Várzea	0.00002	0.00007	0.00008	0.00006	0.00005	0.00005
Iranduba	0.00428	0.00786	0.00948	0.00672	0.00644	0.00690
Itacoatiara	0.00063	0.00039	0.00051	0.00051	0.00052	0.00054
Itapiranga	0.00163	0.00187	0.00220	0.00207	0.00141	0.00206
Manacapuru	0.00083	0.00150	0.00186	0.00128	0.00135	0.00136
Manaquiri	0.00018	0.00022	0.00030	0.00020	0.00024	0.00021
Manaus	0.01073	0.00998	0.01019	0.01155	0.01015	0.01124
Novo Airão	0.00101	0.00213	0.00146	0.00185	0.00154	0.00195
Presidente Figueiredo	0.00140	0.00138	0.00115	0.00150	0.00157	0.00157
Rio Preto da Eva	0.00314	0.00199	0.00262	0.00275	0.00269	0.00267
Silves	0.00032	0.00009	0.00012	0.00022	0.00015	0.00019

Table S-3. Model configuration for the land-use/cover simulation of the MMR. The transitions considered are Forest to Deforestation and Deforestation to Urban Area.

Transition	Calibration period	Validation period	Module Change Matrix	Expander (Patcher)			Comparison year observed vs. simulated map
				Mean Patch Size (Ha)	Patch Size Variance (Ha)	Patch Isometry	
Forest to Deforestation	2004-2010	2012-2017	0.2	5 (5)	10 (0)	1.5 (1.5)	2017
Deforestation to Urban Area	2004-2010	2012-2017	0.9	5 (5)	0 (0)	1.5 (1.5)	
Null model (coefficient values of zero for the weights-of-evidence)							
Forest to Deforestation	2004-2010	2012-2017	0.2	5 (5)	10 (0)	1.5 (1.5)	2017
Deforestation to Urban Area	2004-2010	2012-2017	0.9	5 (5)	0 (0)	1.5 (1.5)	

Table S-4. Deforested area and urban area of protection units, Indigenous lands, and special areas (parks and military areas) for the period from 2020 to 2100 for the MMR.

Deforestation Area (km²)									
Regions	2020	2030	2040	2050	2060	2070	2080	2090	2100
Integral Protection	34.9	419.1	46.4	50.8	57.2	66.7	77.6	92.0	115.4
Sustainable Use	2,030.1	2,534.8	3,002.9	3,432.1	3,835.7	4,200.3	4,521.2	4,797.3	5,040.5
Indigenous Lands	373.9	474.8	581.0	676.0	776.8	881.9	998.0	1,121.3	1,230.5
Special Areas	1.1	1.8	2.5	4.3	6.3	8.3	10.8	13.6	16.0

Urban Area (km²)									
Regions	2020	2030	2040	2050	2060	2070	2080	2090	2100
Integral Protection	0.6	0.6	0.6	0.7	0.7	0.7	0.8	0.8	0.9
Sustainable Use	142.9	206.0	283.5	384.9	504.6	642.7	799.7	980.6	1,186.6
Indigenous Lands	0.2	0.6	1.0	1.8	2.5	3.2	3.9	5.1	6.1
Special Areas	0.06	0.8	1.5	2.0	3.1	3.9	5.0	6.8	9.3

Figure S-1. Forest area rate in municipalities of the MMR from 2017 to 2100 and absolute values in km².

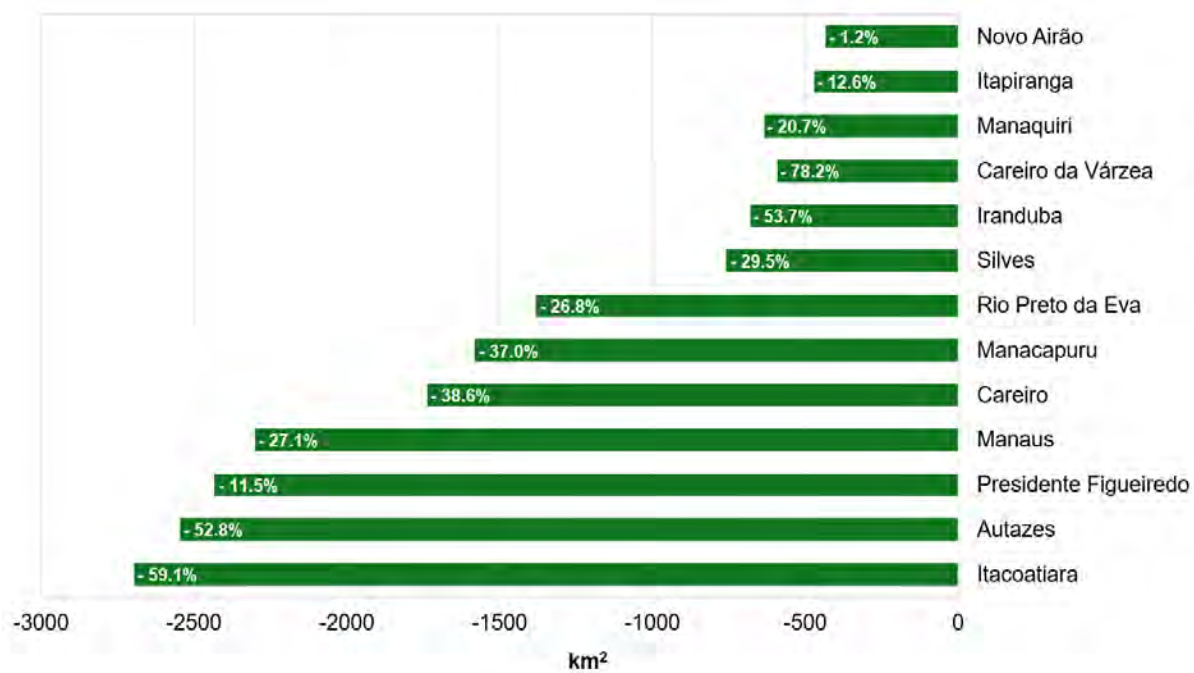


Figure S-2. Map of land use/cover in 2017 and expected change of land use/cover in 2100 for the MMR.

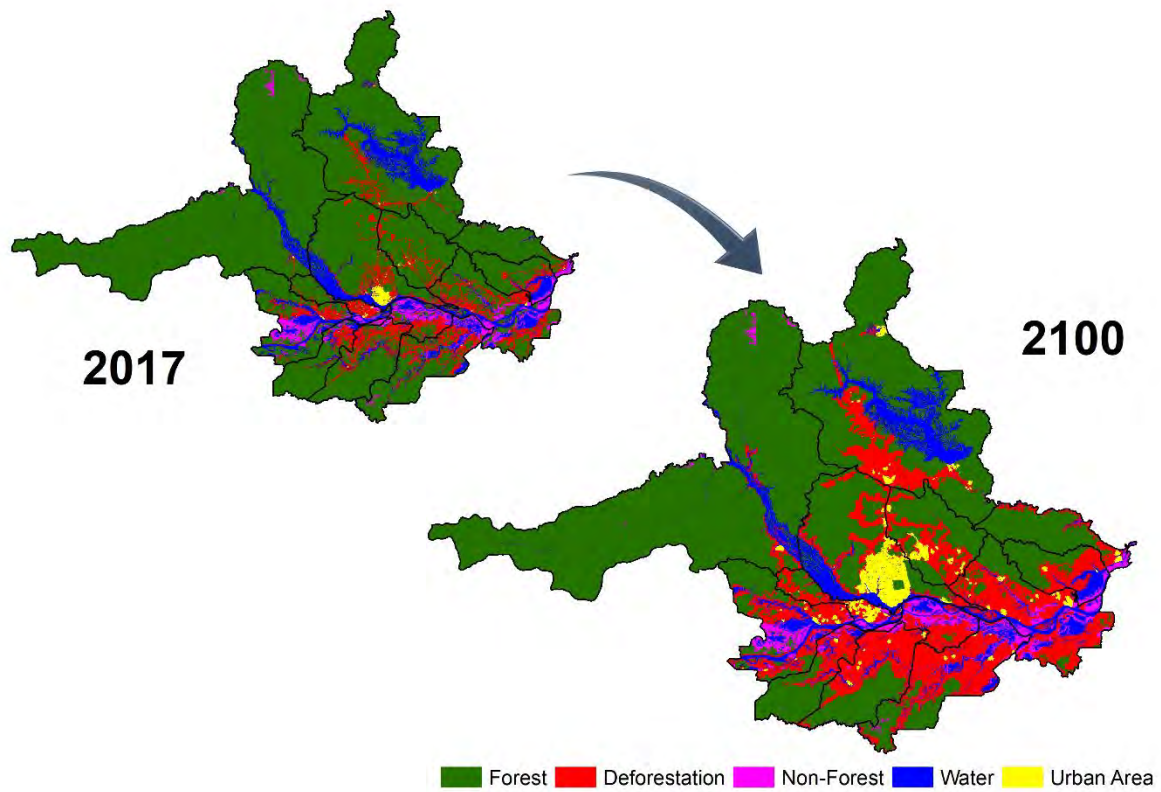


Figure S-3. Values of deforestation rates of increase ($\text{km}^2 \text{year}^{-1}$) for the Legal Amazon region (yellow bar), the state of Amazonas (blue bar), and the MMR municipalities for the period between 2004 and 2017. Sources: PRODES (2019a); PRODES (2019b); INPE (2017).

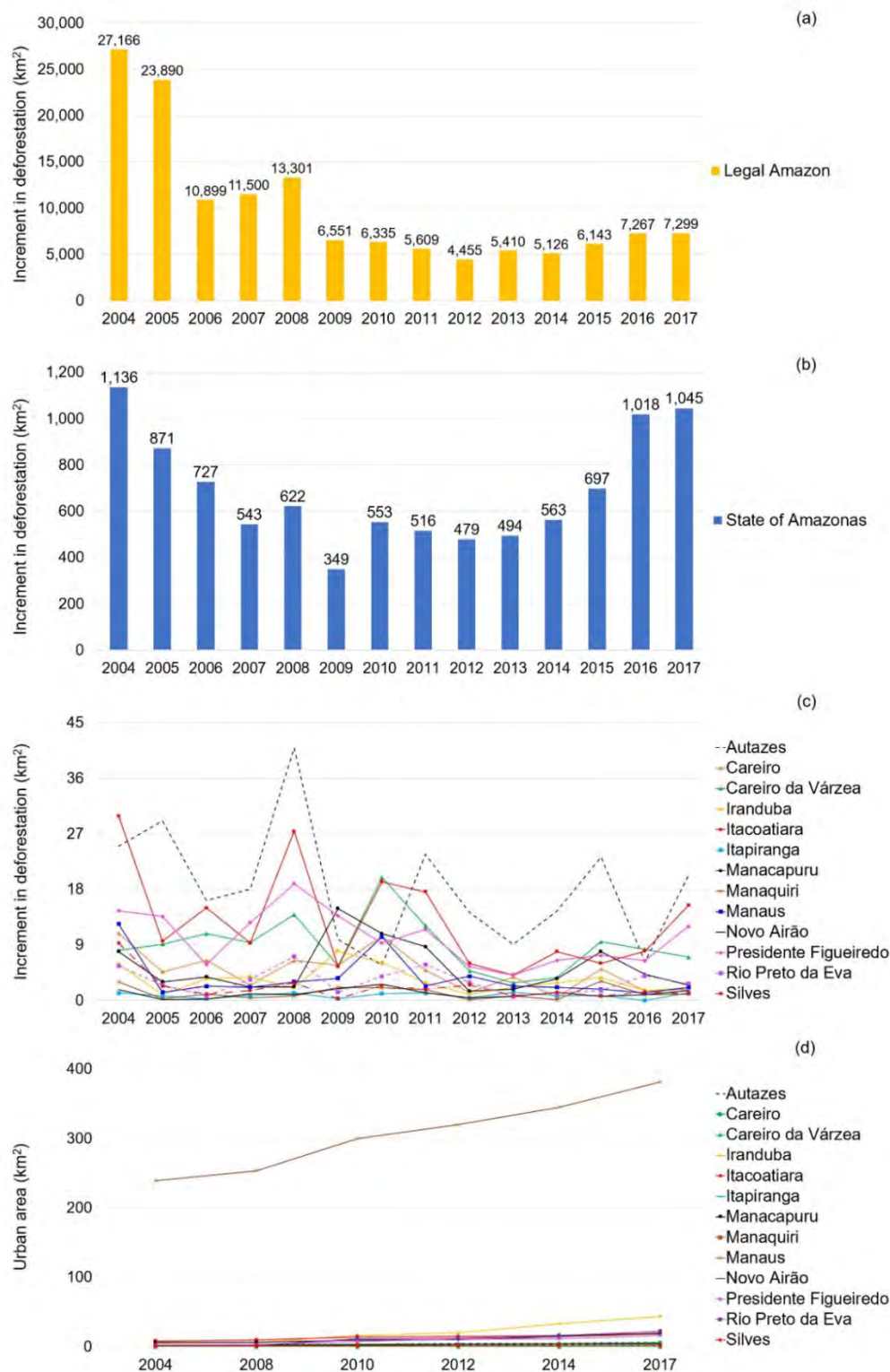
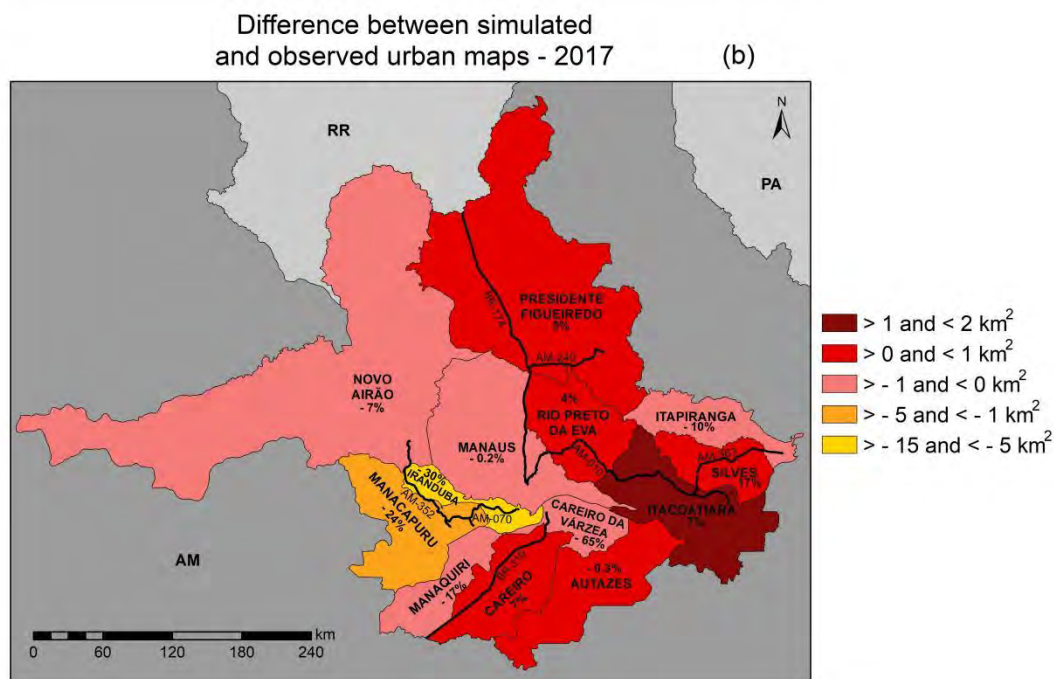
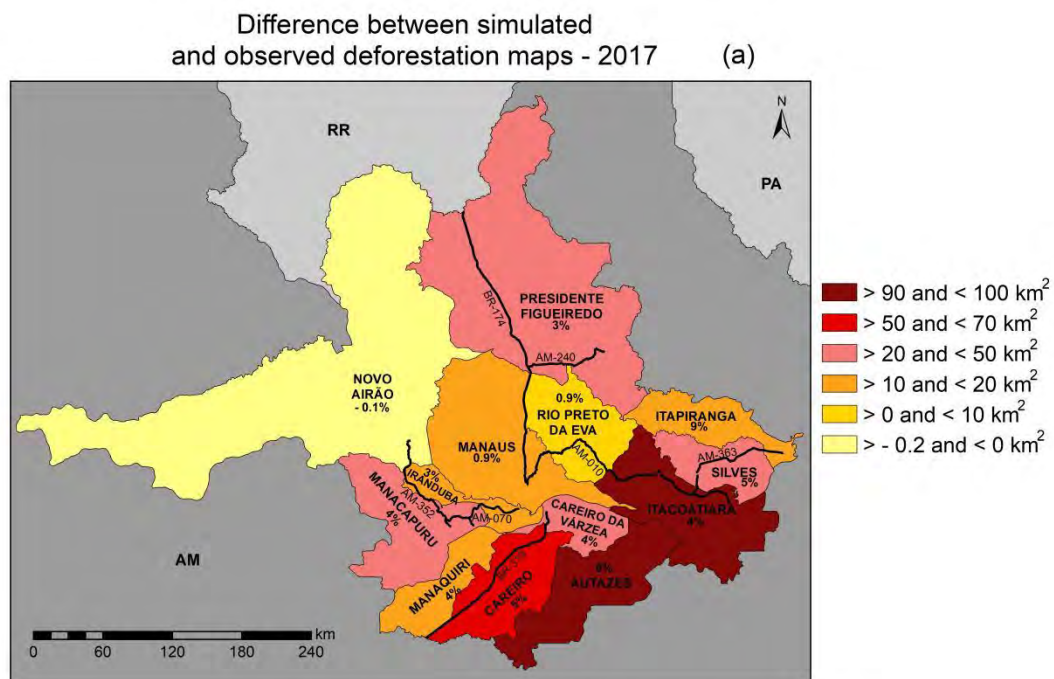


Figure S-4. Spatial distribution of the difference between deforestation areas and urban areas between the observed and simulated 2017 maps for the MMR.



References

- Barni, P. E., Fearnside, P. M., & Graça, P. M. L. A. (2015). Simulating Deforestation and Carbon Loss in Amazonia: Impacts in Brazil's Roraima State from Reconstructing Highway BR-319 (Manaus-Porto Velho). *Environmental Management*, 55(2), 259-278. <https://doi.org/10.1007/s00267-014-0408-6>.
- INPE. (2017). National Institute of Space Research. Centro Regionais da Amazônia. TerraClass. In *Projeto TerraClass 2014*. Retrieved November 10, 2017 from <http://terrabrasilis.dpi.inpe.br/downloads/>.
- Maeda, E. E., Almeida, C. M., Ximenes, A. C., Formaggio, A. R., Shimabukuro, Y. E., & Pellikka, P. (2011). Dynamic modeling of forest conversion: Simulation of past and future scenarios of rural activities expansion in the fringes of the Xingu National Park, Brazilian Amazon. *International Journal of Applied Earth Observation and Geoinformation*, 13(3), 435-446. <https://doi.org/10.1016/j.jag.2010.09.008>.
- PRODES. (2019a). National Institute of Space Research. Desmatamentos nos municípios. Retrieved December 5, 2019 from <http://www.dpi.inpe.br/prodesdigital/prodesmunicipal.php>.
- PRODES. (2019b). National Institute of Space Research. In *TerraBrasilis*. Retrieved October 5, 2019 from http://terrabrasilis.dpi.inpe.br/app/dashboard/deforestation/biomes/legal_amazon/rates.
- Roriz, P. A. C., Yanai, A. M., & Fearnside, P. M. (2017). Deforestation and carbon loss in Southwest Amazonia: impact of Brazil's revised forest code. *Environmental Management*, 60(3), 367-382. <https://doi.org/10.1007/s00267-017-0879-3>.
- Soares-Filho, B. S., Rodrigues, H. O., & Costa, W. L. (2009). *Modeling Environmental Dynamics with Dinamica EGO: Guidebook*. Retrieved October 10, 2017 from <https://csr.ufmg.br/dinamica/dokuwiki/doku.php?id=tutorial:start>
- Teixeira, G. G., & Soares-Filho, B. S. (2018). Simulação da tendência do desmatamento nas Cabeceiras do Rio Xingu, Mato Grosso – Brasil. In: *Anais XIV Simpósio Brasileiro de Sensoriamento Remoto*, Natal, Rio Grande do Norte: Instituto Nacional de Pesquisas Espaciais, São José dos Campos, SP, Brazil. pp. 5483-5490.
- Yanai, A. M., Fearnside, P. M., Graça, P. M. L. A., & Nogueira, E. M. (2012). Avoided deforestation in Brazilian Amazonia: simulating the effect of the Juma Sustainable Development Reserve. *Forest Ecology and Management*, 282, 78-91. <https://doi.org/10.1016/j.foreco.2012.06.029>.